Role of T_0 in CMB anisotropy measurements

Yunfei Wen,[1,2,*] Douglas Scott,[1,†] Raelyn Sullivan,[1,‡] and J. P. Zibin[§]

[1]*Department of Physics & Astronomy University of British Columbia,*
Vancouver, British Columbia V6T 1Z1, Canada
[2]*Department of Applied Mathematics University of Waterloo, Waterloo, Ontario N2L 3G1, Canada*

The quantity T_0, the cosmic microwave background (CMB) monopole, is an often neglected seventh parameter of the standard cosmological model. As well as its variation affecting the physics of the CMB, the measurement of T_0 is also used to calibrate the anisotropies via the orbital dipole. We point out that it is easy to misestimate the effect of T_0 because the CMB anisotropies are conventionally provided in temperature units. In fact the anisotropies are most naturally described as dimensionless and we argue for restoring the convention of working with $\Delta T/T$ rather than ΔT. As a free cosmological parameter, T_0 most naturally only impacts the CMB power spectra through late-time effects. Thus if we ignore the *COBE*-FIRAS measurement, current CMB data only weakly constrain T_0. Even ideal future CMB data can at best provide a percent-level constraint on T_0, although adding large-scale structure data will lead to further improvement. The FIRAS measurement is so precise that its uncertainty negligibly affects most, but not all, cosmological parameter inferences for current CMB experiments. However, if we eventually want to extract all available information from CMB power spectra measured to multipoles $\ell \simeq 5000$, then we will need a better determination of T_0 than is currently available.

I. INTRODUCTION

Experimental results in the past couple of decades have established Λ cold dark matter (ΛCDM) as the standard model of cosmology. This era of precision cosmology has been largely driven by studies of the cosmic microwave background (CMB), which demonstrate that a 6-parameter model provides a good fit to the data. The basic parameter set is often written as $\{\Omega_b h^2, \Omega_c h^2, \theta_*, A_s, n_s, \tau\}$, which has been tightly constrained by *Planck* [1–3] and other experiments [4,5]. Despite this being described as the 6-parameter ΛCDM model, there is in fact a seventh parameter, namely T_0, the present-day temperature of the photon background, or the monopole term in the spherical-harmonic expansion of the CMB sky. This additional parameter is usually neglected because it is so well measured that it can be regarded as effectively fixed.

In current cosmological analyses, T_0 is given by the precise measurements available from a combination of data from *COBE*-FIRAS [6] and other experiments [7], yielding

$$T_{0,\mathrm{F}} = (2.7255 \pm 0.0006) \text{ K}, \tag{1}$$

[*]y52wen@uwaterloo.ca
[†]dscott@phas.ubc.ca
[‡]rsullivan@phas.ubc.ca
[§]zibin@cosm.ca

which has an uncertainty at the level of 0.02%; for simplicity we will refer to this as the "FIRAS" temperature. The *Planck* 2018 results give values of θ_* and $\Omega_b h^2$ that are constrained to approximately the 0.03% and 0.67% levels, respectively [3], which begin to approach the precision of $T_{0,\mathrm{F}}$. In the future, with continuously improving measurements of higher multipoles of CMB power spectra from ground-based experiments [8–10], and the possibility of ambitious space-based experiments [11], it will be possible to approach a cosmic-variance-limited (CVL) measurement for power spectra to high multipoles, particularly for polarization, where there are not expected to be significant small-scale foreground signals. With correspondingly dramatic improvements in the derived cosmological parameters, in this paper we assess whether it is reasonable to continue treating temperature as a constant in the cosmological analysis or whether we will eventually need a better measurement of the CMB monopole in order to fully exploit the constraining power of future experimental data.

Once we start to consider T_0 as a variable, the current way of presenting CMB data in temperature units needs to be reexamined. This is because, besides being a cosmological parameter, T_0 is also used for the calibration and presentation of CMB data. The theoretical power spectra C_ℓ calculated by cosmological codes (e.g., CAMB [12] or CLASS [13]) are frequently presented in temperature units [μK^2]. This is despite the fact that from the time of the earliest discussions of CMB anisotropies, theorists tended

TABLE I.   68% confidence intervals for the 6-parameter base-ΛCDM model from the 2018 *Planck* TT, TE, EE + lowE + lensing likelihood [3,19]. For all the analyses in this paper, we choose the central values of the below intervals as the fiducial model, and we adopt the below error bars as the standard uncertainties for reference. Note that if we use the FIRAS prior in the 7-parameter ΛCDM + T_0 model, we obtain essentially identical results.

$\Omega_b h^2$	$\Omega_c h^2$	$100\theta_*$	$10^9 A_s$	n_s	τ
0.02237 ± 0.00015	0.1200 ± 0.0012	1.04110 ± 0.00031	2.100 ± 0.030	0.9649 ± 0.0042	0.0544 ± 0.0073

to frame their calculations in terms of fractional perturbations, i.e., $\Delta T/T$. This can be seen in early papers by Peebles [14], Sachs and Wolfe [15], Silk [16], and Sunyaev and Zeldovich [17]. Conversely, the results of anisotropy experiments, including both the measured Solar dipole and the measured CMB power spectra, are usually expressed in temperature units. This may seem natural, given that a Planck distribution is fully described by a temperature; however, as we discuss later, the calibration of measurements also has to be considered. As measurements became more precise and the annual variation of the dipole started being used as the primary calibration source, the fact that experiments are directly measuring a dimensionless quantity has become more obscured.

To understand T_0 as a parameter, it is necessary to disentangle the role of T_0 in the calibration process from T_0 in the physics. The situation would be more straightforward if $\Delta T/T$ units were used in presenting data as well as for discussing theoretical predictions. Our purpose here is to clarify these issues in order to ultimately decide whether variations of T_0 within a 7-parameter model actually matter.

In this paper we first review the issue of CMB calibration and discuss the problem of using temperature units for CMB data in Sec. II. In Sec. III, we present a pedagogical argument for the theoretical role of T_0 in a 7-parameter ΛCDM model (primarily building on the work of Ref. [18]), and provide constraints on T_0 from current and future CMB power spectra and other data. Next, in Sec. IV we analyze the impact of the current T_0 uncertainty (from the FIRAS measurement) on cosmological parameter constraints in current and future CMB experiments. We conclude in Sec. V.

Throughout the paper, we use a Fisher-matrix formalism to forecast parameter constraints from CMB data (also including measurements of the baryon acoustic oscillations). The method used and conditions set for our calculations are described in detail in Appendix A. Since we use several different symbols to refer to various definitions of the background temperature, we give a table of definitions for reference in Appendix B. Last, we also discuss the relationship between T_0 and inhomogeneity in Appendix C. Throughout we adopt a fiducial flat ΛCDM model with the parameter values in Table I, from *Planck* [3,19], which represents the smallest uncertainties we currently have for parameters in ΛCDM from CMB data alone. Except where explicitly stated otherwise, all the parameter uncertainties are given as $\pm 1\sigma$, which

corresponds to the 68% confidence interval for a Gaussian distribution.

II. CALIBRATION AND UNITS

A. Motivation for dimensionless fluctuations

The CMB temperature anisotropy power spectrum C_ℓ [which is related to the multipole-scaled quantity $D_\ell = \ell(\ell+1)C_\ell/(2\pi)$] is usually defined as the covariance of the coefficients of the spherical harmonic expansion of the dimensionless quantity $\Delta T(\hat{n})/T$, where $\hat{n}$ is the direction on the sky. The predictions of theoretical models for the power spectra are also most directly obtained as dimensionless quantities. Indeed, the dimensionless anisotropy power is directly related to the dimensionless amplitude of primordial curvature perturbations, A_s, and for the primary anisotropies the dimensionless power (unlike the power in temperature units) satisfies the approximate scaling relation [20]

$$\ell'^2 C_{\ell'}(t') \simeq \ell^2 C_\ell(t) \tag{2}$$

during the evolution of the Universe, where

$$\ell' \equiv \ell \frac{D_A(t')}{D_A(t)}, \tag{3}$$

for angular diameter distance $D_A(t)$ from recombination to the observer at time t. However, in the current convention the temperature and polarization anisotropy power spectra are given in temperature units (usually μK^2) for measured results from CMB experiments and, usually, also for the results of theoretical calculations. On the other hand the lensing reconstruction spectrum, $C_\ell^{\phi\phi}$, is always provided in dimensionless form.

While conventions can be difficult to change, we advocate here for the use of dimensionless quantities exclusively, in both theoretical and experimental studies. Apart from their simpler theoretical properties described above, dimensionless quantities are also advantageous from the standpoint of calibration. All CMB anisotropy experiments use differential measurements, and so they are not directly sensitive to the value of the temperature monopole (but see below for further discussion on this point). In a typical CMB experiment, the detectors measure, in volts, differences between the brightness of positions on the sky. These data then need to be calibrated. The most precise

calibration is the annual time variation of the dipole, often referred to as the "orbital dipole." This is known to extremely high precision (in velocity, or v/c or $\Delta T/T$ units) because of the complete knowledge of the satellite's orbital motion [21]. This calibration then allows the annually averaged dipole (usually called the "Solar dipole") to be extracted from the data, also in dimensionless units. It should be clear that this argument for the $\ell = 1$ mode applies equally well to all the other multipole coefficients of the measured CMB sky, so they too are fundamentally measured in velocity, or dimensionless, units.

To help elucidate the advantages of dimensionless quantities, it will be useful to consider the calibration of CMB anisotropy experiments in more detail; here we focus on the *Planck* satellite, but we expect the same discussion to apply generally. The approaches for the calibration of data from *Planck* are described in great detail in a series of papers [21–27]. For clarity of the treatment, we ignore foregrounds for the moment and assume that only CMB anisotropy is being observed. *Planck* measures a signal (a detector voltage) that (ignoring beam effects, which could easily be added) is proportional to the intensity difference between two directions on the sky,

$$\Delta I_\nu(\nu, \hat{\mathbf{n}}) \equiv I_\nu(\nu, \hat{\mathbf{n}}) - I_\nu(\nu, \hat{\mathbf{m}}) \simeq \frac{dI_\nu}{dT}\bigg|_{\hat{\mathbf{m}}} \Delta T(\hat{\mathbf{n}}) \quad (4)$$

at first order in $\Delta T(\hat{\mathbf{n}})$, where $\hat{\mathbf{m}}$ is a (fixed) reference direction, with $T(\hat{\mathbf{m}}) \equiv T_0$ and $\Delta T(\hat{\mathbf{n}}) \equiv T(\hat{\mathbf{n}}) - T_0$, and $I_\nu(\nu, \hat{\mathbf{n}})$ is the Planck intensity distribution. When *Planck* uses the orbital dipole for calibration, the amplitude of that dipole, $v_{\mathrm{od}}/c = \Delta T_{\mathrm{od}}/T_0$, is known with very high precision. Therefore, according to Eq. (4), at first order in $\Delta T(\hat{\mathbf{n}})$ we have

$$\frac{v_{\mathrm{od}}}{c} = \frac{\Delta I_{\nu,\mathrm{od}}(\nu)}{T_0 dI_\nu/dT|_{\hat{\mathbf{m}}}} = \frac{e^{x_0} - 1}{x_0 e^{x_0}} \frac{\Delta I_{\nu,\mathrm{od}}(\nu)}{I_\nu(\nu, \hat{\mathbf{m}})}, \quad (5)$$

where $\Delta I_{\nu,\mathrm{od}}(\nu)$ is the intensity difference corresponding to the orbital dipole amplitude and $x_0(\nu) \equiv h\nu/(kT_0)$. Therefore the orbital dipole calibration gives directly, at the same precision as we know v_{od}/c, the quantity on the right-hand side of Eq. (5), and *not* the intensity difference $\Delta I_{\nu,\mathrm{od}}/I_\nu$. It is only when we also know T_0 (and hence x_0) precisely that the calibration also gives us $\Delta I_{\nu,\mathrm{od}}/I_\nu$.

Next, when *Planck* measures a CMB fluctuation in some direction $\hat{\mathbf{n}}$, combining Eqs. (4) and (5) gives, at first order,

$$\frac{\Delta T(\hat{\mathbf{n}})}{T_0} = \frac{\Delta I_\nu(\nu, \hat{\mathbf{n}})}{\Delta I_{\nu,\mathrm{od}}(\nu)} \frac{v_{\mathrm{od}}}{c}. \quad (6)$$

Thus we can determine the (dimensionless) temperature fluctuation knowing only the ratio $\Delta I_\nu(\nu, \hat{\mathbf{n}})/\Delta I_{\nu,\mathrm{od}}(\nu)$, which is equal to the (directly measured) corresponding detector voltage ratio. In particular, we do not need to know

T_0, so if the T_0 value we adopted was completely wrong we would still obtain the correct dimensionless $\Delta T(\hat{\mathbf{n}})/T_0$ for the fluctuations.

It may be worth adding that for the two highest frequency channels of *Planck*, where the CMB anisotropies do not dominate even at high Galactic latitudes, the calibration procedure instead uses the brightness of planets. This is most naturally done in intensity units, i.e., ΔI_ν rather than $\Delta T/T$. However, the precision of the planetary calibration process only reaches the 1% level under the most optimistic set of assumptions [28] and hence has no bearing on the details of the much more precise T_0 calibration that we are discussing here.

When we include foregrounds, the total signal is often written in terms of the Rayleigh-Jeans temperature fluctuation, explicitly (see, e.g., [29])

$$\Delta T_{\mathrm{RJ}}(\nu, \hat{\mathbf{n}}) = \frac{x_0^2 e^{x_0}}{(e^{x_0} - 1)^2} \Delta T_{\mathrm{CMB}}(\hat{\mathbf{n}}) + \sum_i A_i(\hat{\mathbf{n}}) F_i(\nu, \hat{\mathbf{n}}, \theta),$$

$$(7)$$

where the sum is over foreground components with amplitudes A_i and frequency dependence F_i, θ is a set of foreground parameters, and the Rayleigh-Jeans temperature fluctuation is given by

$$\Delta T_{\mathrm{RJ}}(\nu, \hat{\mathbf{n}}) = \frac{\Delta I_\nu(\nu, \hat{\mathbf{n}}) c^2}{2k\nu^2}. \quad (8)$$

The relation corresponding to Eq. (6) for the Rayleigh-Jeans temperature fluctuation is

$$\frac{(e^{x_0} - 1)^2}{x_0^2 e^{x_0}} \frac{\Delta T_{\mathrm{RJ}}(\nu, \hat{\mathbf{n}})}{T_0} = \frac{\Delta I_\nu(\nu, \hat{\mathbf{n}})}{\Delta I_{\nu,\mathrm{od}}(\nu)} \frac{v_{\mathrm{od}}}{c}. \quad (9)$$

Again, the quantity on the right-hand side of this equation is directly measured when using the orbital dipole for calibration, and is independent of T_0; however, now we need T_0 if we wish to determine the Rayleigh-Jeans fluctuation. We can nevertheless write Eq. (7) in a form that is dimensionless and independent of the value of T_0 as

$$\frac{(e^{x_0} - 1)^2}{x_0^2 e^{x_0}} \frac{\Delta T_{\mathrm{RJ}}(\nu, \hat{\mathbf{n}})}{T_0}$$
$$= \frac{\Delta T_{\mathrm{CMB}}(\hat{\mathbf{n}})}{T_0} + \frac{(e^{x_0} - 1)^2}{x_0^2 e^{x_0}} \sum_i \frac{A_i(\hat{\mathbf{n}})}{T_0} F_i(\nu, \hat{\mathbf{n}}, \theta). \quad (10)$$

Here the foreground amplitude parameters will have units of temperature, so indeed this expression is dimensionless. Again, we stress that the quantity on the left-hand side is *directly* measured in terms of the calibration, *independently of* T_0, according to Eq. (9).

Now finally, if we imagine a hypothetical situation where our adopted value of T_0 is wrong, the measured left-hand

side of Eq. (10) will not change. However, the T_0- (and ν-) dependent factors multiplying the foreground sum *will* change. To the extent that the foreground parameters are degenerate with this change, we could still recover the correct CMB fluctuations; however, the foreground parameters would be biased from their true values. For a large enough error in our adopted T_0, we expect the shift in T_0 to no longer be degenerate with shifts in foreground parameters, so we would have a poor fit, and might not correctly recover the CMB anisotropies. This is not surprising, considering that using an incorrect value of T_0 means we might be assuming in error that the CMB dominates (or does not) over a particular foreground component in some frequency range. In principle, to the extent that we are confident about which foreground components are important and can place priors on their parameters, Eq. (10) implies that we could place a constraint on T_0 from the *Planck* frequency maps alone. However, for this to be useful, we would need a very precise first-principles calculation of the foreground parameters. In practice such parameters will have fairly wide priors and hence any constraint on T_0 from matching foregrounds will be quite weak.

To summarize, it is the dimensionless CMB fluctuation $\Delta T / T_0$ that is most directly constrained in terms of the orbital dipole calibration. Ignoring foregrounds, we can determine $\Delta T / T_0$ this way independently of the monopole T_0. In the presence of foregrounds, errors in T_0 may bias the foreground parameters, though in practice the uncertainties in those parameters should far exceed the level of the FIRAS T_0 uncertainty.

B. Conversion to temperature units

If we do wish to give the amplitude of the Solar dipole and higher multipoles in temperature units, it is necessary to multiply by a monopole value. Here there are two slightly different questions that we can ask. The first is "what is the best we can say about C_ℓ in temperature units?" If $C_\ell^{[D]}$ is the measured dimensionless spectrum and $C_\ell^{[T]}$ is in temperature units,[1] the answer is

$$C_\ell^{[T]} = T_0^2 C_\ell^{[D]}(T_0, \mathbf{p}), \tag{11}$$

where $\mathbf{p}$ represents the remaining cosmological parameters. The quantity $C_\ell^{[T]}$ in Eq. (11) is equivalent to the covariance of the a_{lm}s when we directly expand $\Delta T(\hat{\mathbf{n}})$ [instead of $\Delta T(\hat{\mathbf{n}})/T$] in spherical harmonics. Here the uncertainty in the FIRAS-derived value $T_{0,F}$ propagates into the uncertainty in $C_\ell^{[T]}$ via the calibration, as it must. Note that, if we

---

[1]Appreciating that it is unorthodox for the units to change the meaning of a variable, here we put the label in square brackets to indicate that we are explicitly referring to a particular choice of units.

wish to compare the measured spectra with model predictions using this conversion method, we must convert both the predicted spectra and the measured spectra (despite the fact that the measured spectra are fundamentally dimensionless in nature) into temperature units, taking account of the uncertainty in T_0. In most practical settings, when we are not considering T_0 to be a free parameter, consideration of the uncertainty in T_0 simply means taking the FIRAS measurement $T_{0,F}$ in Eq. (1).

The second approach to converting the spectra to temperature units is the answer to the question: "what is the best we can say about the anisotropy power?" The answer is now

$$C_\ell^{[T]} = T_c^2 C_\ell^{[D]}(T_0, \mathbf{p}), \tag{12}$$

where T_c is a fixed calibration temperature that we select in order to convert C_ℓ from dimensionless to temperature units. Since T_c is constant [conventionally the central value of the FIRAS measurement, Eq. (1), hereafter $\bar{T}_{0,F}$], the T_0 uncertainty does *not* propagate into the errors in $C_\ell^{[T]}$, and so we know $C_\ell^{[T]}$ with greater precision than if we had used Eq. (11). Of course, when using Eq. (12) there is no actual dependence on the experimental value of the monopole in the calibration, since one could always divide out the fixed value of T_c that was used and recover the original dimensionless measurement. So it is equivalent, but simpler, to stay dimensionless from the start. Another potential problem with choosing a factor T_c is that a future measurement of T_0 [30,31] might give a different central value, complicating comparisons.

In practice with current experiments, it makes essentially no difference which calibration approach we take as far as the higher multipoles ($\ell \geq 2$) are concerned, since the FIRAS uncertainty is negligible compared to other errors. However, for the Solar dipole, folding in the FIRAS error does make a substantial contribution to the total uncertainty. In this case, when quoting the results in velocity units the Planck Collaboration papers never include the FIRAS error. However, the situation is not always consistent when it comes to presenting the uncertainty of the Solar dipole in temperature units and choosing whether to add the FIRAS uncertainty in quadrature [21,26,27,32,33]. Nevertheless, in their latest results [33,34] the collaboration does include the FIRAS uncertainty in the temperature-units dipole. The resulting inflation of uncertainties should be taken into account when comparing different dipole measurements. In summary, *Planck* uses both approaches listed above for converting the dipole amplitude to temperature units. While neither approach is wrong (since they provide answers to slightly different questions), we consider that the second approach of choosing fixed T_c, without combining the FIRAS error, is the more appropriate one. This is because it correctly reflects the

dimensionless nature of the dipole measurement and more accurately summarizes our current knowledge of the Solar dipole uncertainty.

Although when comparing the results of higher multipoles in present-day experiments with theoretical calculations it makes essentially no difference whether one uses temperature units or dimensionless quantities, there *are* situations in which this distinction can be crucial. In particular, when considering a 7-parameter $\Lambda\text{CDM} + T_0$ model, with variable background temperature, we should calculate the theoretical dimensionless power spectra by varying T_0 along with the usual cosmological parameters, but we should *not* include the T_0 variation in the calibration of the power spectra. In other words, we should use Eq. (12) instead of Eq. (11). If we used Eq. (11) (and did not similarly scale the calibration of the measured spectra we compare with), the variation of T_0 would cause an additional change of the overall amplitude of the power spectra, which would lead to a strong degeneracy between T_0 and A_s. In addition, the fact that the lensing spectrum $C_\ell^{\phi\phi}$ is always presented in dimensionless form can lead to an artificially strong lensing constraint [18]. As seen in Fig. 1 using a Fisher-matrix analysis (see Appendix A for

more details), the incorrect calibration method leads to a much larger uncertainty on A_s, due to the T_0-A_s degeneracy, and a significantly smaller uncertainty on T_0, due to the artificial effect on lensing. Indeed, the incorrect-calibration error on A_s is dominated by that of T_0 at large $\ell_{\max}$, as expected given the T_0-A_s degeneracy.

This issue with the temperature calibration of theoretical CMB power spectra was a problem [35,36] in Refs. [11,37], and affected the results in the latter reference since it found that the uncertainty on A_s increased substantially when including T_0 as a parameter. It was also a problem in version 1 of Ref. [18], which led to an unrealistically tight predicted constraint on T_0 from CMB anisotropies.

In summary, since the CMB power spectra are most naturally dimensionless in theory and are also measured directly in $\Delta T/T$ units, there is no compelling need to present the spectra in temperature units. The current convention is simply one of convenience. For clarity of the physical meaning of the quantities being calculated and measured and for the sake of uniformity across power spectra, it would be better to present all future results as dimensionless quantities. In the rest of this paper, for all our analyses, we will follow Eq. (12), the second approach, whenever we need to calculate C_ℓ in temperature units to meet the current convention.

III. T_0 IN COSMOLOGICAL MODELS

With the clarification of temperature calibration in Sec. II, it is clear that when we discuss changing T_0 in a 7-parameter ΛCDM model, we should only consider its impact on the dimensionless CMB power spectra $C_\ell^{[\text{D}]}$ in Eq. (12). The investigation of the effects of varying T_0 on the CMB power spectra goes back at least to the paper by Hu *et al.* in 1995 [38] and was further developed about 12 years later [39,40], with the constraining power of CMB power spectra on T_0 first explored using *Planck* anisotropy data in Sec. 6.7.3 of Ref. [2]. However, it is only through the recent papers by Ivanov *et al.* [18] and Bose and Lombriser [41] that the role of T_0 as a cosmological parameter has been more fully explored.

A. The role of T_γ

The temperature of the background photons, T_γ, is a function of time or redshift, with $T_\gamma(z = 0) = T_0$. One can consider several different quantities to trace the evolution of the cosmological model, including scale factor a, redshift z, cosmological (or proper) time t, and Hubble parameter H. As a dynamical variable, T_γ plays a similar role, and can be used as an alternative quantity to set the timescale. One can imagine different observers living in a particular Friedmann universe but observing the CMB at different times [20,42], with the observed T_0 as one way of fixing the epoch.

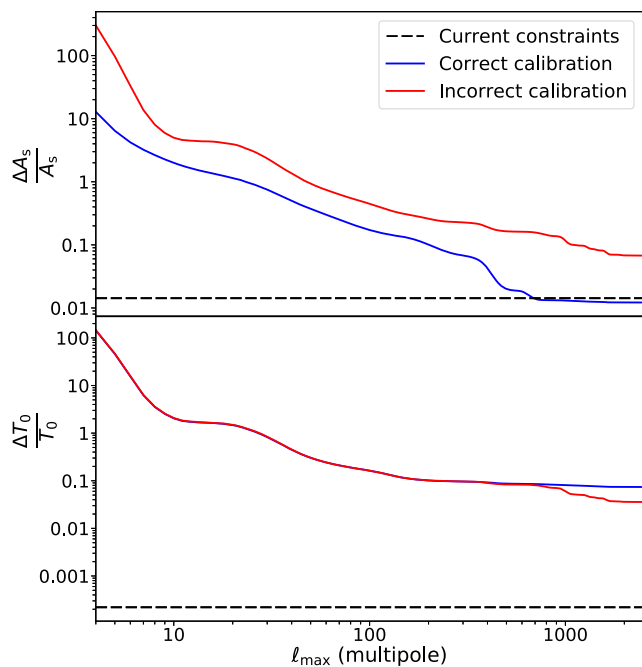T_γ also traces the overall radiation content of the Universe, which includes other light species that evolve

FIG. 1. Predicted uncertainties on the power spectrum amplitude parameter A_s and the CMB monopole temperature T_0 using lensed TT, TE, and EE power spectra. Including noise at the level of the *Planck* experiment, we show the relative error estimate for T_0 and A_s with respect to the maximum ℓ, with both the correct [Eq. (12)] and incorrect [Eq. (11)] temperature calibration procedures (as described in Sec. II) for the 7-parameter $\Lambda\text{CDM} + T_0$ model. The horizontal black dashed lines give the uncertainty in A_s derived from the actual 2018 *Planck* TT, TE, EE + lensing likelihood and the uncertainty from the FIRAS T_0 measurement.

in the same way as photons, often parameterised with N_{eff}. Important epochs, such as nucleosynthesis or recombination, are set by a comparison between fundamental physical quantities (e.g., particle number densities, masses, and couplings) and the radiation content in the background cosmological model, which is set by T_γ. This "clock" can be made manifestly dimensionless (see Ref. [43]) by defining the quantity $\Theta = kT_\gamma/m_p c^2$, the ratio of thermal energy to proton mass.

In the ΛCDM model, the expansion history of the Universe is determined by the energy densities of baryons ρ_b, cold dark matter ρ_c, radiation ρ_r, and dark energy ρ_Λ, most of which vary with time. To relate the densities at a specific epoch with the present-day cosmological parameters $\Omega_b h^2$, $\Omega_c h^2$, and T_0, we have, for example,

$$\rho_b = \rho_{b,0} a^{-3} = \rho_{b,0}(T_0/T_\gamma)^{-3} \propto \frac{\Omega_b h^2}{(T_0/\bar{T}_{0,F})^3} T_\gamma^3. \quad (13)$$

We can set $\tilde{\omega}_b = \Omega_b h^2(T_0/\bar{T}_{0,F})^{-3}$, where $\bar{T}_{0,F}$ (the central value of the FIRAS measurement; see Appendix B) is used to allow easy comparison between the 6- and 7-parameter ΛCDM models, such that when $T_0 = \bar{T}_{0,F}$, then $\tilde{\omega}_b = \Omega_b h^2$. According to Eq. (13), $\rho_b \propto \tilde{\omega}_b T_\gamma^3$, and, similarly, we can define $\tilde{\omega}_c = \Omega_c h^2(T_0/\bar{T}_{0,F})^{-3}$, so that $\rho_c \propto \tilde{\omega}_c T_\gamma^3$. The radiation density ρ_r is sufficiently described by T_γ and N_{eff} (we take $N_{\text{eff}} = 3.046$ here). Therefore, when we use T_γ as the timescale, the expansion history H of the early Universe can be written as a function of $\tilde{\omega}_b$, $\tilde{\omega}_c$, and T_γ only, with dark energy negligible at early times.

The redefined present-day cosmological parameters $\tilde{\omega}_b$ and $\tilde{\omega}_c$ can be used as alternatives to $\Omega_b h^2$ and $\Omega_c h^2$ in a 7-parameter extension of ΛCDM with T_0 as a free variable. In fact, $\tilde{\omega}_b$ and $\tilde{\omega}_c$ in ΛCDM $+ T_0$ play a similar role to $\Omega_b h^2$ and $\Omega_c h^2$ in 6-parameter ΛCDM. Using a Fisher-matrix analysis with TT, TE, and EE power spectra (as described in Appendix A), we can see in Fig. 2 that with negligible instrumental noise and perfect removal of foreground signals (i.e., the CVL assumption) the constraints we obtain for $\tilde{\omega}_b$ are essentially the same in the two models. Although still quite similar, there is some noticeable difference for $\tilde{\omega}_c$, due to the effects of lensing. As seen in Fig. 2, the $\tilde{\omega}_c$ constraints for the two models begin to differ at $\ell_{\text{max}} \simeq 1000$ and then start to converge again at $\ell_{\text{max}} \simeq 4000$. This behavior can be explained by the transition between different lensing effects: lensing smoothing, which dominates out to ℓ of a few thousand, and extra small-scale power, which dominates the spectra at higher ℓ, as diffusion damping wipes out the primary power spectra [44]. The parameter $\tilde{\omega}_c$ exhibits much stronger degeneracy with T_0 in the lensing-smoothing regime than does $\tilde{\omega}_b$, thereby weakening the constraining power of $\tilde{\omega}_c$ in ΛCDM $+ T_0$. This degeneracy is removed in the small-scale lensing power regime, providing additional
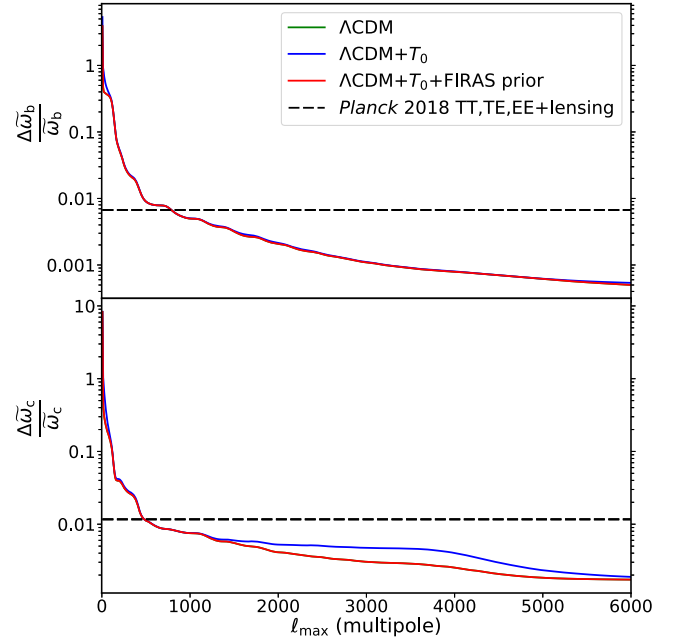

FIG. 2. Forecast constraints on $\tilde{\omega}_b$ and $\tilde{\omega}_c$ as a function of the maximum multipole considered. We specifically give the forecasts with negligible instrumental noise (i.e., the cosmic-variance limit, described in Appendix A) from a combination of CMB TT, TE, and EE power spectra for several different assumptions. The blue curve shows the constraints for a 7-parameter ΛCDM model with T_0 as a free variable. The red curve shows the constraints for a 7-parameter ΛCDM model, with T_0 having a FIRAS prior [i.e., following Eq. (1)]. The green curve shows the constraints for the standard 6-parameter ΛCDM model, where $\tilde{\omega}_b = \Omega_b h^2$ and $\tilde{\omega}_c = \Omega_c h^2$. The green curve completely overlaps with the red curve, which means that when applying the FIRAS prior, there is no discernible difference for $\tilde{\omega}_b$ and $\tilde{\omega}_c$ between the 6- and 7-parameter models. The blue curve basically follows the red curve for $\tilde{\omega}_b$, while there is some noticeable difference between the two curves for $\tilde{\omega}_c$. This difference can be explained by the impacts of lensing smoothing and small-scale lensing power (see text).

constraining power for $\tilde{\omega}_c$, independent of T_0. While the uncertainty on $\tilde{\omega}_c$ is clearly impacted by opening up T_0 as a free parameter, since the difference between the $\tilde{\omega}_c$ constraints of the two models is relatively small in such a CVL setting, we can for the most part regard $\tilde{\omega}_c$ as a replacement for $\Omega_c h^2$ in a 7-parameter ΛCDM $+ T_0$ model. For the other four standard cosmological parameters, namely $\{\theta_*, A_s, n_s, \tau\}$, the forecast errors for each parameter only increase slightly by changing T_0 from a constant to a free parameter under the CVL assumption.

B. Recombination physics and T_0

During the major events of the early Universe (such as nucleosynthesis and recombination), the physical processes are largely determined by the number densities of electrons and baryons, as well as the energy density of cold dark matter, together with the expansion history (which at very

early times is predominantly driven by the radiation component). With the known average mass of a baryon, we can use ρ_b as a proxy for the associated number density, so that $\rho_b \propto \tilde{\omega}_b T_\gamma^3$, $\rho_c \propto \tilde{\omega}_c T_\gamma^3$, and T_γ are the only relevant background quantities in the ΛCDM model determining the progress of decoupling of particle interactions. From such a qualitative argument, it is already clear that all the physical processes in the early Universe are set by $\tilde{\omega}_b$ and $\tilde{\omega}_c$, without explicit dependence on T_0. Indeed this notion that recombination depends only on physics local to last scattering was the basis of the use of effective models, with varying T_0, to calculate CMB spectra in models with large underdensities in Ref. [45]. Nonetheless, we will now offer a more detailed discussion of the process of recombination and the epoch of last scattering (since they are of utmost importance to CMB power spectra) as examples to further illustrate the idea.

Cosmological recombination is described by a set of coupled first-order differential equations for the free electron fraction X_e, the electron temperature T_e,[2] and the photon phase-space density, with respect to proper time t [47–50]. Using the differential relation

$$dt = \frac{dt}{da}\frac{da}{dT_\gamma}dT_\gamma = -\frac{1}{HT_\gamma}dT_\gamma, \quad (14)$$

which does not explicitly depend on T_0, we can rewrite the governing differential equations for recombination in terms of T_γ [18]; it is then clear that the recombination history $X_e(t)$ is determined only by the parameters $\tilde{\omega}_b$, $\tilde{\omega}_c$, and T_γ, along with physical constants.

The differential Thomson optical depth for recombination is given by

$$\dot{\tau}_{\rm rec} = \frac{d\tau_{\rm rec}}{dt} = c\sigma_T n_H(T_\gamma, \tilde{\omega}_b)X_e(T_\gamma, \tilde{\omega}_b, \tilde{\omega}_c), \quad (15)$$

where c is the speed of light, σ_T is the Thomson cross section, and n_H is the number density of hydrogen atoms, which can be converted to ρ_b with a fixed helium fraction. We use the subscript "rec" to distinguish the optical depth coming from the recombination process from the small optical depth coming from the reionization parameter τ in ΛCDM. The optical depth for recombination out to some specific epoch is then simply

$$\tau_{\rm rec} = \int_t^{t_0} \dot{\tau}_{\rm rec}(t')dt' = \int_{T_0}^{T_\gamma} \frac{1}{T_\gamma' H}\dot{\tau}_{\rm rec}(T_\gamma')dT_\gamma',$$

$$= c\sigma_T \int_{T_0}^{T_\gamma} \frac{n_H(T_\gamma', \tilde{\omega}_b)X_e(T_\gamma', \tilde{\omega}_b, \tilde{\omega}_c)}{T_\gamma' H(T_\gamma', \tilde{\omega}_b, \tilde{\omega}_c)}dT_\gamma', \quad (16)$$

where t_0 is the current proper time.

There are two common approaches for defining the epoch of last scattering t_* (or similarly z_* or T_*). The first approach is to define it to correspond to the peak of the visibility function $g(t) = \dot{\tau}_{\rm rec}\exp(-\tau_{\rm rec})$ (e.g., Ref. [51]). The peak condition $dg(t_*)/dt = 0$ yields

$$\frac{d\dot{\tau}_{\rm rec}(t_*)}{dt} = \dot{\tau}_{\rm rec}^2(t_*). \quad (17)$$

Recasting this in terms of T_γ, we obtain a precise definition of the last-scattering temperature T_*. Since both dt/dT_γ and $\dot{\tau}_{\rm rec}$ are independent of T_0, then T_* is only a function of $\tilde{\omega}_b$ and $\tilde{\omega}_c$, without any explicit T_0 dependence.

The second approach is to define the last-scattering epoch to correspond to the time back to when the optical depth reaches unity, i.e., $\tau_{\rm rec}(t_*) = \tau_{\rm rec}(T_*) = 1$ (e.g., Refs. [3,12,52]). In this case, at least in principle, $\tau_{\rm rec}$ does depend on T_0 through the lower bound of the integration in Eq. (16); however, this dependence is extremely weak, since X_e (excluding the effect of reionization) is only of order 10^{-4} at the current epoch, thereby giving negligible contribution to $\tau_{\rm rec}$ during the late-time evolution of the Universe [20]. We numerically assessed the degree of this weak T_0 dependence, finding that with either a fixed integrand in Eq. (16) or a fixed θ_* value (detailed definition of the parameter θ_* is given in Sec. III D),[3] a 15% change of T_0 around $\bar{T}_{0,F}$ leads to no discernible change in T_*. For all practical purposes, we can therefore consider T_* to be independent of T_0 in Eq. (16). In practice, both these definitions of the last-scattering epoch yield almost the same results, with the calculated results for T_* (or z_*) under the two approaches coinciding within 5×10^{-4} in a fiducial model near the current measurement of cosmological parameters [52]. We adopt the second approach in this paper for the definition of the last-scattering epoch to allow for later comparison with *Planck* results.

Using a Markov-chain Monte Carlo (MCMC) method with the 2018 *Planck* TT, TE, EE + lensing likelihood in a 7-parameter ΛCDM + T_0 model, we find that $T_* = 2970.9^{+0.8}_{-1.0}$ K, which is constrained extremely well, to 0.03%. This is consistent with the ΛCDM T_* value, as expected based on the above physical arguments that T_* depends only on conditions local to last scattering; however, it contradicts the claim of a changing temperature at last scattering in the ΛCDM + T_0 model made in Ref. [53]. Coincidentally the uncertainty of T_* is comparable to that of the FIRAS result on T_0 in Eq. (1). In contrast to this, we

---

[2]T_e is very close to T_γ at early times, differing only at the level of 10^{-7} during recombination [46].

[3]We briefly compare the two methods used to assess the impact of T_0 on T_* in Eq. (16). Since T_0 only appears as the lower bound of the integration, the obvious method is to fix the integrand while varying T_0, which corresponds with changing the current observation epoch in the same Friedmann model. However, as discussed in Sec. III D, it is more physical to fix θ_* when we analyze the impact of T_0 under CMB power spectra constraints, so we actually performed the check using both methods.

find $z_* = 936 \pm 60$, with a relatively large uncertainty. Such great uncertainty is mainly due to the weak constraint on T_0 from CMB power spectra, which will be further discussed in Sec. III C. In the standard 6-parameter ΛCDM model, the relative uncertainty on z_* is the same as that on T_*. Nevertheless, we can see that, when allowing T_0 to be a free parameter, the physics more directly constrains the value of T_* than z_* from recombination. As established in Fig. 2, $\tilde{\omega}_b$ and $\tilde{\omega}_c$ are constrained by CMB power spectra to almost the same accuracy in a 7-parameter ΛCDM $+ T_0$ model as $\Omega_b h^2$ and $\Omega_c h^2$ are in 6-parameter ΛCDM. With the current *Planck* likelihood, $\tilde{\omega}_b$ and $\tilde{\omega}_c$ are constrained to the percent level (see the dashed lines in Fig. 2), in contrast to the 0.03% accuracy for T_*. Compared to the baryon and cold dark matter densities, the temperature at last scattering is much more tightly constrained, since the last-scattering epoch T_* (or z_* in ΛCDM) is generally a weak function of cosmological parameters [54].

With T_* as an extremely well measured quantity, then the baryon and cold dark matter densities at last scattering, $\rho_b(T_*) \propto \tilde{\omega}_b T_*^3$ and $\rho_c(T_*) \propto \tilde{\omega}_c T_*^3$, are in fact relatively well constrained by CMB power spectra. Some of the papers in the literature discussing T_0 as a free parameter seem to suggest that T_0 directly impacts recombination [11,39,53]. This is mainly due to directly varying T_0 without considering $\tilde{\omega}_b$ and $\tilde{\omega}_c$ as new variables. If one simply fixes $\Omega_b h^2$ and $\Omega_c h^2$, while changing T_0, then the baryon and matter densities at the recombination epoch are actually changed, which drastically alters the recombination history [39]. However, baryon and dark matter densities at last scattering are actually fairly well measured through recombination physics, so such an approach of fixing $\Omega_b h^2$ and $\Omega_c h^2$ and changing T_0 does not correspond with the constraint conditions set by CMB power spectra. A better and more physically motivated approach for analyzing the effects of T_0 on cosmology is to fix $\tilde{\omega}_b$ and $\tilde{\omega}_c$, which are well constrained in the 7-parameter ΛCDM $+ T_0$ model.

When analyzing the impact of varying T_0 in cosmological models, it is crucial to distinguish T_0 from T_*, based on their roles in recombination. The dynamical variable T_γ clearly enters recombination physics, with T_* being set by the absolute energy scale of atomic and particle physics and well determined by CMB power spectra; however, the present-day background photon temperature T_0 only serves as a relative timescale that indicates how much the Universe has expanded since the time of last scattering, with T_0 itself having no effect on the physics of the early Universe when using the physically relevant parameters $\tilde{\omega}_b$ and $\tilde{\omega}_c$.

C. Constraining T_0 with CMB power spectra

As established in Sec. II, the calibration of CMB anisotropy data does not actually involve the current experimentally determined CMB monopole, T_0. Nevertheless, if T_0 impacts the dimensionless C_ℓ, then in principle we can provide an independent constraint on T_0 from the measured (dimensionless) anisotropy power spectra.

Since the *shapes* of the primary CMB anisotropy power spectra are determined by the physical conditions around the last-scattering epoch (on which T_0 has no impact when $\tilde{\omega}_b$ and $\tilde{\omega}_c$ are used as density parameters), they only tell us about the physical conditions at recombination and provide no constraints on T_0. Nevertheless, changing T_0 does alter the amount of expansion after the last-scattering epoch, changing the angular-diameter distance D_A back to the recombination epoch, which shifts the anisotropies in multipole space. However, the angular scale of the acoustic oscillations is actually extremely tightly constrained by CMB experiments [3]. Therefore, as we vary T_0, we have to take advantage of the geometrical degeneracy and change the values of other cosmological parameters in order to preserve the angular acoustic scale (as discussed further in the next section). As a result, the acoustic oscillations in the power spectra, both in shape and period, give no information about the epoch at which we are observing.

By contrast, secondary anisotropies, generated after the last-scattering epoch, can break this degeneracy and provide some constraints on T_0. In particular as structure forms and dark energy starts to dominate at low redshifts, both the so-called integrated Sachs-Wolfe (ISW) effect [15] and gravitational lensing depend on the late-time expansion and give observable imprints on the CMB anisotropies, and hence their signatures are able to constrain T_0. To quantify these effects, we calculate the predicted T_0 constraints using lensed TT, TE, and EE power spectra through a Fisher-matrix analysis (see Appendix A). We can see in Fig. 1 that as ℓ_{max} is increased, there is a substantial drop in the uncertainty on T_0 until $\ell_{max} \simeq 30$ (which is where the ISW effect contributes) and a continuous decrease towards higher multipoles (where gravitational lensing contributes).

Using the 2018 *Planck* TT, TE, EE + lensing likelihood, we find the 68% interval to be $T_0 = 3.10^{+0.18}_{-0.09}$ K and the 95% interval to be $T_0 = 3.11^{+0.22}_{-0.25}$ K, with the distribution of T_0 values shown in Fig. 3. Our results were found using an MCMC analysis with the COBAYA [55] and CAMB [12] codes, with RECFAST [56,57] included for the recombination modeling. These results are in excellent agreement with those in Ref. [18], which used a different set of cosmological codes. As seen in Fig. 3, this constraint depends strongly on the priors imposed on the underlying cosmology, most prominently the assumption that the dark energy should be positive, i.e., $\Omega_\Lambda \geq 0$. For models with negative dark energy T_0 can go as high as 3.8K, and the associated uncertainty on T_0 becomes significantly larger, with a 1σ value around 0.2K, which agrees with the blue line in Fig. 1 determined by the Fisher forecast. In general, the current *Planck* data provide a poor constraint on T_0. Since $\tilde{\omega}_b$ and $\tilde{\omega}_c$ are as well constrained in a 7-parameter ΛCDM $+ T_0$ model as $\Omega_b h^2$ and $\Omega_c h^2$ are in the
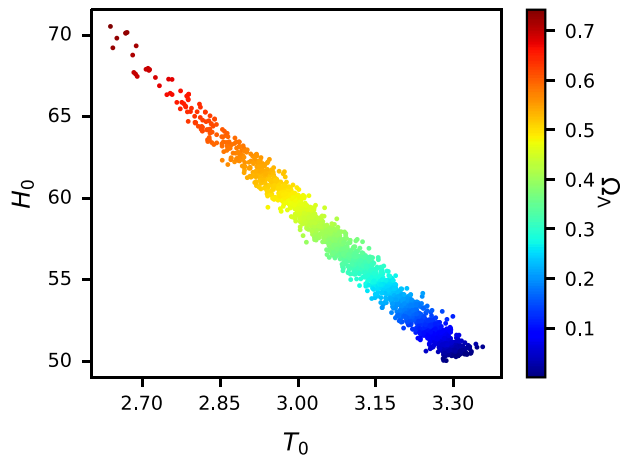
FIG. 3. Samples from MCMC posteriors using the 2018 *Planck* TT, TE, EE + lensing likelihood for the 7-parameter ΛCDM + T_0 model, plotted in the T_0-H_0 plane and color coded by the value of Ω_Λ. The degeneracy between T_0 and H_0 is clearly seen in the plot, with Ω_Λ corresponding to different amounts of late-time expansion and late-ISW effects. The current constraint on T_0 from the *Planck* dataset is highly dependent on the prior choice, with $\Omega_\Lambda \geq 0$ imposed here.

FIG. 4. Predictions of the level of uncertainty on T_0 as a function of maximum multipole, coming from CMB anisotropy power spectra, under the cosmic-variance limit (described in Appendix A). The purple (dot-dashed) curve corresponds to the use of unlensed *TT*, *TE*, and *EE* power spectra (although unrealistic, they are plotted here to assess the size of the different physical effects), the blue (dashed) curve is for the lensed *TT*, *TE*, and *EE* power spectra, and the red (solid) curve uses the lensed *TT*, *TE*, and *EE* power spectra as well as the lensing-reconstruction power spectrum $C_\ell^{\phi\phi}$. For comparison, the black line shows the uncertainty of the FIRAS measurement.

6-parameter ΛCDM model, the weak constraint on T_0 leads to considerable degeneracy between T_0 and $\Omega_b h^2$ and between T_0 and $\Omega_c h^2$ [2].

As seen above, the central value of the T_0 constraint from the *Planck* 2018 data is about 2σ higher than the FIRAS measurement. This slight shift is mainly caused by the twin facts that the low multipoles ($\ell \lesssim 30$) in the measured *TT* power spectrum of *Planck* are somewhat low compared to the best-fit ΛCDM model and that the observed *TT* power spectrum appears to be more smoothed by lensing than expected (as usually characterized by the consistency parameter A_L) [3]. Both the "low-ℓ deficit" and "A_L tension" have already been shown to have an impact on the standard parameter constraints [3,58]. With a higher T_0 value, the theoretical *TT* power spectra prefer less large-scale power and more lensing smoothing [18], which both correspond with the direction of the deviation in the observed data. Since T_0 is only constrained by late-ISW and lensing effects, the low-ℓ deficit and A_L tension lead to a small shift in the parameter constraint on T_0, resulting in this 2σ deviation from the FIRAS result.

Figure 4 demonstrates the predicted constraining power on T_0 coming from CMB power spectra for an ideal CMB experiment (described in Appendix A). With negligible instrumental noise, gravitational lensing provides a much stronger constraint on the amount of late-time Universe expansion compared to the constraint coming from *Planck*; this is because the temperature and polarization power spectra for $\ell \gtrsim 1000$ (where lensing smoothing plays a major role) and the lensing reconstruction spectrum $C_\ell^{\phi\phi}$ are much better measured in an ideal experiment, while the
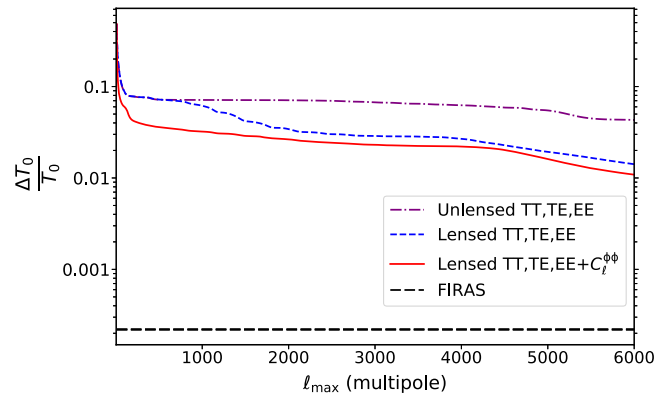
late-ISW effect is limited by the high cosmic variance at low ℓ. In general, lensing decreases the uncertainty on T_0 (out to $\ell_{\max} \simeq 6000$) by around a factor of 4 compared with the late-ISW effect. The lensing smoothing effect starts to become important at $\ell \gtrsim 1000$ as expected, and additionally the lensing reconstruction spectrum drives down the T_0 uncertainty mainly around $\ell \simeq 100$, where the peak of $C_\ell^{\phi\phi}$ is located. Changes in cosmological parameters mainly lead to a shift of the overall amplitude for $C_\ell^{\phi\phi}$ (rather than a change in the shape [59]), so the peak region provides most of the constraining power for any parameter. Combining both lensing smoothing and lensing reconstruction leads to an improvement in the T_0 constraint by a small amount. However, even the most ideal CMB experiment is only able to constrain T_0 to around 0.03 K, which is still about two orders of magnitude poorer than the FIRAS measurement. This means that we will never be able to obtain a competitive constraint on T_0 from CMB anisotropy data alone, compared to FIRAS.

It *is* possible to obtain a better constraint on T_0 by combining CMB anisotropy data with other cosmological data sets. Reference [2] has already noted that combining baryonic acoustic oscillation (BAO) data [60] with the full 2015 *Planck* likelihood leads to a 68% confidence interval of $T_0 = (2.718 \pm 0.021)$ K, and we find a similar result when combining the *Planck* 2018 likelihood with current BAO data. Unlike the constraint from *Planck* data alone, this measurement is not shifted high, but is completely compatible with the FIRAS measurement. Because T_0 is effectively a parameter measuring the amount of expansion

since recombination, any measurement of the late-time Universe that constrains the expansion history should strengthen the constraint on T_0. With the error from the noise-free CMB data alone also predicted to be at around the 1% level, one might expect to obtain an independent T_0 measurement with a precision comparable to the current FIRAS uncertainty level by combining future CMB anisotropy experiments with upcoming large-scale structure (LSS) surveys such as DESI [61] and *Euclid* [62].

To give a simplistic assessment of this idea, we combine the Fisher forecast from *TT*, *TE*, *EE*, and lensing reconstruction spectra in an ideal CMB anisotropy experiment (shown in Fig. 4) with the forecast from measurements of the BAO scale in a *Euclid*-like survey [63]. Details of our BAO forecast method are given in Appendix A. The combination of CMB and BAO data is predicted to constrain T_0 with an uncertainty of around 0.006K, which is about four times better than the constraint from ideal CMB alone, or the constraint from a combination of *Planck* and current BAO data. Even though 0.006K is an order of magnitude less constraining than the FIRAS measurement, the CMB anisotropy plus BAO constraint will nonetheless provide a relatively precise measurement of T_0 that is independent of FIRAS. In principle, we could further drive down the uncertainty on T_0 with the full constraining power of a *Euclid*-like experiment by including galaxy clustering and weak lensing measurements in addition to BAO data. However, determining such future predictions from LSS data is outside the scope of this paper. Still, from our discussion of the role of T_0 and our simple combination of future BAO and ideal CMB anisotropy constraints, it is already clear that combining next-generation CMB and LSS data will offer an independent measurement of T_0 with a precision that could approach that of FIRAS. Whether such a constraint will ever surpass the current FIRAS error remains to be seen.

D. T_0 and other cosmological parameters

Since CMB data alone only provide a weak constraint on T_0, through the late-ISW and lensing effects, it is possible to connect T_0 variation with other cosmological parameters. For example Ivanov *et al.* [18] focus on the tension between CMB-derived [3] and distance-ladder-derived estimates of the Hubble constant [64]. Although they conclude that changing T_0 does not provide a viable solution to this apparent cosmological parameter discrepancy, it is nevertheless instructive to see how the parameter degeneracies work here.

In the standard ΛCDM model, θ_*, which is the ratio between the proper sound horizon at recombination ($d_s^* = a_* r_s$) and the angular-diameter distance back to the recombination epoch (D_A), is the best constrained parameter from CMB experiments due to the well-measured acoustic oscillations of the CMB power spectra [3]. The angular-diameter distance to the last-scattering epoch can be written as

$$
\begin{aligned}
D_A &= \frac{1}{(1+z_*)} \int_0^{z_*} \frac{cdz}{H(z, \Omega_m, \Omega_\Lambda)}, \\
&= \frac{1}{T_*} \int_{T_0}^{T_*} \frac{cdT_\gamma}{H(T_\gamma, H_0, \tilde{\omega}_b, \tilde{\omega}_c)},
\end{aligned}
\tag{18}
$$

where we neglect the radiation, neutrino, and curvature background components for simplicity, since the effects of these components on the expansion history are relatively small compared to the impacts of varying T_0 within the weak T_0 constraint from *Planck*. Reference [18] demonstrates that $d_s^* = (T_0/T_*)r_s$ is only a function of $\tilde{\omega}_b$ and $\tilde{\omega}_c$, without explicit dependence on T_0. Therefore, since $\tilde{\omega}_b, \tilde{\omega}_c$, and θ_* are measured significantly better through CMB power spectra compared to T_0, we can regard $\tilde{\omega}_b, \tilde{\omega}_c$, and θ_* as fixed here, so that T_*, d_s^*, and D_A can also be considered to be fixed. Viewed as an integral with respect to T_γ, D_A can now be treated as a function of only two variables (namely T_0 and H_0) whose combination in some functional form gives a fixed value. Hence, T_0 and H_0 have an approximate degeneracy when $\tilde{\omega}_b, \tilde{\omega}_c$, and θ_* are measured so well compared to the poor constraint on T_0 coming from CMB power spectra. This T_0-H_0 degeneracy can be best seen in Fig. 3 with samples from an MCMC run. The uncertainty on T_0 physically corresponds with the uncertainty on the amount of dark energy contained in the Universe, which is demonstrated by the variation of Ω_Λ along the T_0-H_0 degeneracy line in the plot. Since θ_* is well measured by CMB experiments, we need to change the amount of dark energy in the Friedmann model to compensate for the change of T_0, in order to obtain a fixed D_A value.

It might be tempting to relate this T_0-H_0 degeneracy to the Hubble-constant tension. Reference [18] finds $T_0 = (2.56 \pm 0.05)$ K by combining *Planck* 2018 data with SH0ES, where the H_0 measurement from the distance ladder provides an additional constraint on the late-time expansion. However, such a result deviates from the current best measurement $T_{0,F} = (2.7255 \pm 0.0006)$ K by hundreds of σ in terms of the FIRAS uncertainty. Therefore, addressing the Hubble tension by varying T_0 requires us to completely discount the FIRAS measurement. One should remember that FIRAS measured the entire frequency spectrum of the CMB, rather than just a single value of the absolute intensity, with the shape of this spectrum determining the value of T_0; hence it is hard to imagine how the derived value of T_0 could be so far off. Moreover, the experimental determination of T_0 does not come entirely from FIRAS, since there have been many other measurements of the CMB monopole temperature. Although the current 0.02% uncertainty in T_0 is dominated by data from FIRAS, there are other independent measurements with uncertainties that are still impressively small [65,66]. Reference [7] provides an alternative estimate from a compilation of measurements excluding FIRAS, $T_0 = (2.729 \pm 0.004)$ K, which still has approximately 0.1%

precision (and is in excellent agreement with the FIRAS constraint). Therefore, the reasonable range of variation of T_0 that is consistent with experimental constraints has an entirely negligible effect on H_0, with or without the *COBE*-FIRAS data. Indeed, since both are background variables, we would expect to require a temperature shift with a magnitude on the order of the Hubble parameter discrepancy, i.e., we would expect $\Delta T_0/T_0 \sim \Delta H_0/H_0 \sim 10\%$, for the Hubble tension to be resolved with a shift in T_0.

On the other hand, since the constraint on T_0 coming from the CMB power spectra arises because of the late-ISW and lensing effects, there *will be* degeneracies between T_0 and other cosmological parameters in some extensions of standard ΛCDM. With *Planck* 2018 data, allowing T_0 to be a free parameter can slightly relieve the so-called A_L tension [41], since varying T_0 also changes the amount of lensing smoothing. Because the spatial curvature parameter Ω_K, the total neutrino mass $\sum m_\nu$, and the dark energy equation of state parameter w also contribute to the late-time expansion of the Universe (and therefore have a direct impact on the late-ISW effect and lensing [37,41,67]), these parameters will also be somewhat correlated with T_0. For a counterexample, the parameter N_{eff} (the effective number of light particle species) only matters when neutrinos are relativistic in the early Universe and so will not be correlated with T_0. Nevertheless, even in cases where there is some degeneracy, the actual uncertainty in the measured T_0 is so small that there is no way of using a shift in T_0 to resolve any apparent parameter tensions.

IV. IMPACT OF FIRAS UNCERTAINTY

A. Current CMB anisotropy experiments

Despite our pedagogical discussion on the role of T_0 as a free variable in Sec. III, any realistic treatment of temperature as a variable requires the adoption of the FIRAS measurement as a prior, representing our current knowledge of T_0. To fold in this information, we will adopt a Gaussian distribution with central value $\bar{T}_{0,\text{F}} = 2.7255$ K and standard deviation $\sigma_{\text{F}} = 0.0006$ K as the prior on T_0. The conventional belief is that the FIRAS measurement does not make any appreciable difference to the current CMB results. This is true for the constraints on the base parameters of ΛCDM, as well as most other parameters. However, as seen in Table II, we noticeably underestimate the error for some of the derived parameters by ignoring the FIRAS uncertainty. Even for present-day anisotropy experiments, the FIRAS prior can have some unexpected impacts on our parameter constraints.

The parameter θ_{MC} is a common alternative to θ_* used in the literature [2,3,5], which is much faster to compute. It is based on a numerical approximation for θ_*, derived in Ref. [54], with the assumption of T_0 being a constant. However, the error on θ_{MC} increases substantially (and a large bias develops) when we vary T_0 as a free parameter

TABLE II. 68% intervals for some derived parameters using the 2018 *Planck* TT, TE, EE + lensing likelihood in an MCMC analysis. We specifically look at θ_{MC} (which we compare with θ_*), z_* and T_* (the redshift and temperature at the last-scattering epoch), and z_{drag} and T_{drag} (the redshift and temperature of the Compton drag epoch). The middle column is for the ΛCDM model with T_0 fixed at 2.7255K, while the last column represents the parameter error on the ΛCDM + T_0 model with the adoption of the FIRAS prior. The errors in the middle column ("T_0 fixed") excluding those for T_* and T_{drag} are presented in the final results of the Planck Collaboration [3].

Parameter	T_0 fixed	FIRAS prior
$100\theta_{\text{MC}}$	1.04092 ± 0.00031	1.04091 ± 0.00037
$100\theta_*$	1.04110 ± 0.00031	1.04111 ± 0.00030
z_*	1089.92 ± 0.25	1089.91 ± 0.34
T_* [K]	2973.27 ± 0.67	2973.28 ± 0.67
z_{drag}	1059.94 ± 0.30	1059.94 ± 0.37
T_{drag} [K]	2891.60 ± 0.78	2891.60 ± 0.78

without the FIRAS prior. The approximating formula for θ_{MC} depends explicitly on $\Omega_b h^2$ and $\Omega_c h^2$ instead of $\tilde{\omega}_b$ and $\tilde{\omega}_c$, and therefore performs poorly when we start to vary T_0. Even when we only vary T_0 within the FIRAS prior, the 68% error of θ_{MC} still increases by about 20% compared to the error with the fixed T_0 model (as seen in Table II). However, the constraint on θ_*, the accurate version of θ_{MC} (as defined in Sec. III D), experiences no statistically significant change with or without fixing T_0. There is no compelling reason to continue using this approximate parameter θ_{MC} in any case, given the currently available computing power.

A similar increase in the uncertainties can also be seen for z_* and z_{drag} (the redshifts at the last-scattering epoch and the Compton-drag epoch, respectively) in Table II. Since CMB power spectra directly constrain T_* to an accuracy comparable to the FIRAS measurement (as established in Sec. III B) instead of z_*, the inclusion of the FIRAS error on T_0 will noticeably increase the error on z_*, considering the relation $z_* = T_*/T_0 - 1$. A similar argument to our discussion on the epoch of last scattering will apply to T_{drag} and z_{drag}, which describe the time of decoupling of baryons from the photon background. Such an underestimation of parameter uncertainties by neglecting the FIRAS error will not occur if we choose to use T_* and T_{drag} instead of z_* and z_{drag} in the first place. It is therefore better to use temperature to describe the timeline of major events in the early Universe rather than redshift.

B. Future CMB anisotropy experiments

Even though the FIRAS error does not make a difference to the main parameter constraints or our actual cosmological model in the current generation of CMB experiments (and will not even for the next generation of "Stage 4" experiments), there is still the question of whether the

FIRAS measurement will be sufficient for *all* the cosmological results of all future CMB experiments. In the rest of this section, we will assess the impact of the FIRAS prior on a CVL CMB experiment going out to high multipoles. A similar question was addressed in Refs. [40,68]; however, Ref. [40] incorrectly propagated the dipole error into the parameter analysis and only considered spectra up to $\ell_{max} = 2500$. Reference [68] focused on a *Planck*-like experiment and also considered the effect of the cosmic variance of T_0; we will discuss this work further in Appendix C.

We now examine the effects of including the FIRAS prior on the constraints of the standard-ΛCDM parameters $\{\Omega_b h^2, \Omega_c h^2, \theta_*, A_s, n_s, \tau\}$ using ideal CVL CMB data. The uncertainties for $\{\theta_*, A_s, n_s, \tau\}$ are different by less than 0.1% in the two settings; hence these can be considered to be unchanged for all practical purposes. However, as shown in Table III and Fig. 5, the constraints for $\Omega_b h^2$ and $\Omega_c h^2$ are noticeably different, with $\Omega_b h^2$ showing the greatest change among all parameters. Using a fixed temperature (i.e., ignoring the FIRAS uncertainty) would lead us to underestimate the error for $\Omega_b h^2$ by around 50% and the error for $\Omega_c h^2$ by around 10% for $\ell_{max} \simeq 6000$. Therefore, for an ideal future experiment, the FIRAS uncertainty *does* have an effect on the standard-model 6-parameter constraints; nevertheless, such differences are modest in size, and in practice any differences would be even smaller because of the inclusion of realistic noise from the instrument and foreground residuals. We can conclude that imposing the FIRAS prior on T_0 will be sufficient for analyzing all CMB experiments in the near future, until such time as we can approach the cosmic-variance limit out to multipoles of many thousands. It is therefore generally safe to continue the practice of treating T_0 as a constant, without any measurable impact on the derived parameters in standard cosmological models. We also checked the effect of adding the lensing reconstruction spectrum $C_\ell^{\phi\phi}$ in the Fisher matrix calculation, and our results still hold (although the uncertainties are slightly smaller).

When we use the alternative parameter set with $\tilde{\omega}_b$ and $\tilde{\omega}_c$, the parameter constraints from the 7-parameter
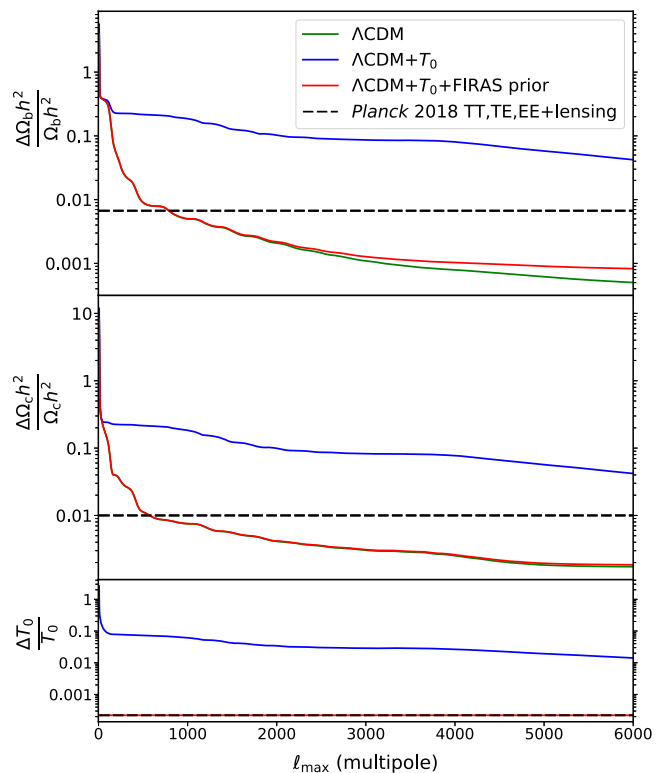

FIG. 5. Estimated Fisher-matrix uncertainties for $\Omega_b h^2$, $\Omega_c h^2$, and T_0 as a function of the maximum ℓ, using lensed TT, TE, and EE power spectra under the assumption of the cosmic-variance limit, as described in Appendix A. The green and blue curves show the constraints for the free 6- and 7-parameter models, respectively. The red curve shows the constraints for a 7-parameter ΛCDM $+ T_0$ model while imposing the FIRAS prior [i.e., following Eq. (1)] on T_0. The horizontal black dashed lines give the uncertainties of $\Omega_b h^2$ and $\Omega_c h^2$ derived from the actual 2018 *Planck* TT, TE, EE $+$ lensing likelihood, along with the uncertainty from the FIRAS T_0 measurement.

ΛCDM $+ T_0$ model with a FIRAS prior are essentially the same as those from the 6-parameter ΛCDM model under CVL conditions forecasted using a Fisher matrix formalism, as shown through the perfectly overlapping green and red curves in Fig. 2. Since $\Omega_b h^2 \propto \tilde{\omega}_b T_0^3$ and $\Omega_c h^2 \propto \tilde{\omega}_c T_0^3$, then the relative errors on $\Omega_b h^2$ and $\Omega_c h^2$ with the FIRAS prior are simply given by those with fixed T_0 added in quadrature with three times the FIRAS uncertainty. The FIRAS uncertainty plays a significant role when the constraints on the parameters $\Omega_b h^2$ (or $\tilde{\omega}_b$) and $\Omega_c h^2$ (or $\tilde{\omega}_c$) approach the FIRAS relative error. This can be seen in Fig. 5, where the constraint on $\Omega_b h^2$ begins to deviate at around $\ell_{max} \simeq 2000$, with the relative error approaching 10^{-3}. Because $\Omega_b h^2$ is constrained by high-ℓ data, the FIRAS uncertainty leads to a more significant effect and eventually causes the 50% underestimation of the error at $\ell_{max} \simeq 6000$. The errors on $\Omega_c h^2$ for the two models also begin to slightly differ in Fig. 5 as the relative error approaches 10^{-3}, for ℓ_{max} extending to 6000. However,

TABLE III. Estimated uncertainties for $\Omega_b h^2$ and $\Omega_c h^2$ from a 7-parameter Fisher-matrix calculation using the lensed TT, TE, and EE power spectra, assuming that we are in the cosmic-variance limit. The second column is for T_0 fixed at 2.7255 K, while the third column is for adoption of the FIRAS prior. In this calculation, we go to $\ell_{max} = 3000$ for the TT power spectrum and $\ell_{max} = 6000$ for the TE and EE power spectra. More details are given in Appendix A.

Parameter	T_0 fixed	FIRAS prior
$\Omega_b h^2$	1.12×10^{-5}	1.85×10^{-5}
$\Omega_c h^2$	2.09×10^{-4}	2.22×10^{-4}

TABLE IV. Estimated uncertainties for some derived parameters from a 7-parameter Fisher-matrix calculation using the lensed TT, TE, and EE power spectra, assuming that we are in the cosmic-variance limit. These estimates are the absolute uncertainties on the parameter (instead of the percentage error). This table is the CVL forecast version of Table II. In this calculation, we go to $\ell_{\text{max}} = 3000$ for the TT power spectrum and $\ell_{\text{max}} = 6000$ for the TE and EE power spectra. More details are given in Appendix A.

Parameter	T_0 fixed	FIRAS prior
$100\theta_{\text{MC}}$	6.0×10^{-5}	2.4×10^{-4}
$100\theta_*$	6.0×10^{-5}	6.0×10^{-5}
z_*	0.021	0.20
T_* [K]	0.056	0.056
z_{drag}	0.033	0.24
T_{drag} [K]	0.090	0.090

since $\Omega_c h^2$ is not as well constrained by CMB anisotropy data as $\Omega_b h^2$, the FIRAS uncertainty impacts the constraints on $\Omega_b h^2$ much more than those on $\Omega_c h^2$. To summarize, the FIRAS uncertainty will have a small (but non-negligible) effect only when $\Omega_b h^2$ and $\Omega_c h^2$ are constrained to about the 0.1% level in ΛCDM.

Following Sec. IV A, we also forecast the uncertainties on the derived cosmological parameters listed in Table II, assuming ideal CMB data in the 6-parameter ΛCDM model. As shown in Table IV, in the cosmic-variance limited setting, the inclusion of the FIRAS error for T_0 increases the uncertainties on θ_{MC}, z_*, and z_{drag} substantially compared to Table II with *Planck* data. In fact, ignoring the FIRAS error underestimates the uncertainties by almost an order of magnitude. This provides compelling evidence that for future CMB analysis we should adopt θ_*, T_*, and T_{drag} as more appropriate parameters that are not sensitive to the change of T_0, compared with their currently used counterparts.

We also examine the effects of including the FIRAS prior on the parameter constraints for some models that are extensions to 6-parameter ΛCDM. In general, the FIRAS prior has negligible impact on these extended parameters in an ideal CVL anisotropy experiment. To illustrate this we take Ω_K as an example of such an extended parameter. As seen in Table V, the inclusion of the FIRAS uncertainty has a similar impact on $\Omega_b h^2$ and $\Omega_c h^2$ for the ΛCDM $+ \Omega_K$ model compared to the results in Table III for ΛCDM; this means that our previous discussion on the impact of the FIRAS uncertainty on the ΛCDM model still holds in this case. Varying Ω_K as a free parameter increases the error in a substantial way only for $\Omega_c h^2$, due to the degeneracy between the matter density and curvature. However, including the FIRAS uncertainty does not impact the error on Ω_K, since the constraint for Ω_K obtained in a CVL CMB anisotropy experiment is still far from the relative accuracy of the FIRAS measurement. Including a *Euclid*-like

TABLE V. Estimated uncertainties for $\Omega_b h^2$, $\Omega_c h^2$, and Ω_K from an 8-parameter ΛCDM $+ \Omega_K + T_0$ model Fisher-matrix calculation using the lensed TT, TE, and EE power spectra, assuming that we are in the cosmic-variance limit. The calculation setting is the same as for Table III, with more details given in Appendix A.

Parameter	T_0 fixed	FIRAS prior
$\Omega_b h^2$	1.13×10^{-5}	1.85×10^{-5}
$\Omega_c h^2$	5.29×10^{-4}	5.35×10^{-4}
Ω_K	1.29×10^{-3}	1.29×10^{-3}

measurement of the BAO scale (see Appendix A for details) further strengthens the parameter constraints, but the FIRAS error still has no impact on the accuracy of Ω_K. Because the FIRAS measurement is so precise, the uncertainty on T_0 will generally not be a concern for future CMB anisotropy experiments placing constraints on the ΛCDM $+ \Omega_K$ model, or on other common extensions to 6-parameter ΛCDM.

C. Future LSS measurements

For ideal CMB anisotropy experiments, we saw that the FIRAS uncertainty starts to inhibit parameter constraints when the errors of $\Omega_b h^2$ and $\Omega_c h^2$ approach the 0.1% level. For upcoming LSS surveys, the uncertainties on some cosmological parameters might also approach this precision. For example, with the combined cosmological probes from galaxy clustering and weak lensing in an optimistic scenario, *Euclid* is projected to constrain several cosmological parameters (including σ_8, h, Ω_b, and Ω_m) to well below the percent level [62], where the present-day uncertainty on T_0 could actually play a role. A more rigorous assessment is needed to determine whether the uncertainty of T_0 will actually matter in practice for such LSS surveys.

V. CONCLUSIONS

In this paper, we have investigated the effect of the parameter T_0 on CMB anisotropies. In order to clarify the role of T_0 in calibration, we advocate the use of dimensionless (i.e., $\Delta T/T$) units to measure, analyze, and present the CMB dipole, as well as the higher multipoles of the CMB sky. When calibrating with the orbital dipole, the dimensionless CMB fluctuations can be measured independently of our knowledge of T_0, even in the presence of foregrounds. The value $T_c = \bar{T}_{0,\text{F}} = 2.7255$ K is merely a particular choice of calibration constant for unit-conversion purposes. Even though dimensionless units and T_c-calibrated temperature units are physically equivalent, it is in principle better to use dimensionless quantities for CMB data, since this avoids unnecessary confusion between T_0 and T_c and prevents people from folding additional temperature uncertainty into the cosmological results. Since the

CMB power spectra are naturally dimensionless in theory and are also measured directly in $\Delta T/T$ units, we should go back to the tradition of using dimensionless units, as theorists did in the earliest discussions of CMB anisotropies.

We have also given an overview of the role of T_0 as a cosmological parameter, building on the work of Refs. [18,41]. As a cosmic clock, T_γ indicates the change of absolute energy scale as the Universe evolves, while $T_0 = T_\gamma(z = 0)$ characterizes the amount of expansion after recombination, a process that is relatively well determined by the primary anisotropies. Clarifying some previous confusion on the role of T_0, we emphasize that the monopole temperature T_0 does not influence the physics of the early Universe, in particular recombination, when holding fixed the parameters $\tilde{\omega}_b$ and $\tilde{\omega}_c$, which are physically relevant at that time and are well constrained. As a result, the constraining power of T_0 from CMB power spectra only comes from late-time effects, in particular the ISW effect and gravitational lensing, with both the lensing smoothing effect on the 2-point functions and the lensing reconstruction spectrum itself providing comparable constraining power. Current CMB anisotropy data give only a weak constraint on T_0, which leads to various degrees of degeneracy between T_0 and other cosmological parameters, including H_0. However, employing such degeneracies to address cosmic tensions ignores the fact that it would require excursions hundreds of times the size of the FIRAS uncertainty to make a substantial difference. This means we would have to disregard current reliable knowledge of T_0, derived not just from *COBE*-FIRAS, but from many other experiments. Using a Fisher-matrix analysis for an ideal future experiment, we estimate that CMB data alone can at best constrain T_0 to the 1% level, which is still two orders of magnitude less constraining than the current local temperature measurements. Adding *Euclid*-like BAO results to the parameter forecasts improves the T_0 constraint by another factor of 4. It is in principle possible to obtain an independent measurement of T_0 with a precision that could approach that of FIRAS by combining future CMB and LSS data.

Despite the pedagogical discussion of treating T_0 as a free variable, we are in the situation where it is sufficient to use the FIRAS measurement as a prior in order to provide any realistic assessment of the impact of T_0 on parameters extracted from CMB power spectra. The FIRAS uncertainty is so small that we can say it will generally have negligible impact on the main cosmological results coming from current and next-generation CMB anisotropy experiments. Hence adopting the central FIRAS value as T_0 will be sufficient for any currently proposed experiment. Nevertheless, it is important to keep in mind that neglecting the error of the FIRAS measurement will noticeably underestimate the uncertainties for several occasionally quoted derived parameters, even in current CMB experiments, although such effects can be mitigated by choosing alternative derived parameters that are less sensitive to the change of T_0. As experimental capabilities improve, the FIRAS uncertainty will eventually impact the constraints on $\Omega_b h^2$ and $\Omega_c h^2$ for the main cosmological parameters as well. In the CVL situation, we will underestimate the uncertainty on $\Omega_b h^2$ by 50% and on $\Omega_c h^2$ by 10% (out to $\ell_{max} = 6000$ for polarization and 3000 for temperature) if we ignore the FIRAS uncertainty on T_0. This shows that if we ultimately want to extract all available information from the CMB power spectra measured to multipoles $\ell \simeq 5000$, then we will indeed need a better determination of T_0 than is currently available. Our work thereby provides another motivation for the proposed future CMB spectral distortion experiments [69–71], which will further improve the accuracy of our measurement for T_0 compared to FIRAS.

APPENDIX A: FISHER-MATRIX METHOD

The Fisher-matrix formalism is a well established tool for forecasting parameter constraints in cosmology [77–80]. We use this approach to assess the impact of varying T_0 on CMB power spectra in both realistic and CVL conditions. For any observed data vector $\mathbf{x}$ and model parameters $\mathbf{p}$, with likelihood function $L(\mathbf{x}; \mathbf{p})$, the Fisher information matrix is defined as

$$\mathsf{F}_{ij} = -\left\langle \frac{\partial^2 \ln L}{\partial p_i \partial p_j} \right\rangle. \tag{A1}$$

By the Cramer-Rao inequality, the variance of an unbiased estimator for a parameter p_i from the data has a lower bound $(\mathsf{F}^{-1})_{ii}$, to which the maximum likelihood estimator approaches asymptotically. Therefore, the Fisher matrix gives an estimate for the approximate error bars achievable from an experiment.

1. Fisher matrix for CMB

The Fisher matrix for CMB temperature and polarization anisotropies is [81,82]

$$\mathsf{F}_{ij}^{\mathrm{CMB}} = \sum_{\ell=2}^{\ell_{\max}} \sum_{X,Y} \frac{\partial C_\ell^X}{\partial p_i} (\mathrm{Cov}_\ell)_{XY}^{-1} \frac{\partial C_\ell^Y}{\partial p_j}, \qquad (\mathrm{A2})$$

assuming Gaussian primordial perturbations and Gaussian noise. C_ℓ^X represents the power of the ℓth multipole for $X = \mathrm{T, E, C}$, which stand for either the lensed or unlensed TT, EE, or TE power spectra, respectively. We neglect the BB power spectrum, since the detection of the primordial signal is not guaranteed and, as we have confirmed, adding the BB power spectrum does not significantly change our results.[4] We use CAMB for all the CMB power spectrum calculations, with RECFAST chosen as the recombination code; we checked that selecting other recombination codes does not impact any of our results. The symmetric covariance matrix Cov_ℓ has elements

$$(\mathrm{Cov}_\ell)_{\mathrm{TT}} = \frac{1}{\mathcal{N}} (C_\ell^{\mathrm{T}} + \omega_{\mathrm{T}}^{-1} B_\ell^{-2})^2, \qquad (\mathrm{A3})$$

$$(\mathrm{Cov}_\ell)_{\mathrm{EE}} = \frac{1}{\mathcal{N}} (C_\ell^{\mathrm{E}} + \omega_{\mathrm{P}}^{-1} B_\ell^{-2})^2, \qquad (\mathrm{A4})$$

$$(\mathrm{Cov}_\ell)_{\mathrm{CC}} = \frac{1}{2\mathcal{N}} [(C_\ell^{\mathrm{C}})^2$$
$$+ (C_\ell^{\mathrm{T}} + \omega_{\mathrm{T}}^{-1} B_\ell^{-2})(C_\ell^{\mathrm{E}} + \omega_{\mathrm{P}}^{-1} B_\ell^{-2})], \quad (\mathrm{A5})$$

$$(\mathrm{Cov}_\ell)_{\mathrm{TE}} = \frac{1}{\mathcal{N}} (C_\ell^{\mathrm{C}})^2, \qquad (\mathrm{A6})$$

$$(\mathrm{Cov}_\ell)_{\mathrm{TC}} = \frac{1}{\mathcal{N}} C_\ell^{\mathrm{C}} (C_\ell^{\mathrm{T}} + \omega_{\mathrm{T}}^{-1} B_\ell^{-2}), \qquad (\mathrm{A7})$$

$$(\mathrm{Cov}_\ell)_{\mathrm{EC}} = \frac{1}{\mathcal{N}} C_\ell^{\mathrm{C}} (C_\ell^{\mathrm{E}} + \omega_{\mathrm{P}}^{-1} B_\ell^{-2}), \qquad (\mathrm{A8})$$

where we define $\mathcal{N} = f_{\mathrm{sky}}(2\ell + 1)/2$, and we take the sky coverage fraction $f_{\mathrm{sky}} = 0.7$ throughout the paper (so in this sense our estimates have some degree of realism, even though we neglect any complications related to foreground removal). The beam window function B_ℓ^2 is assumed to be Gaussian with $B_\ell^2 = \exp[-\ell(\ell+1)\theta_{\mathrm{beam}}^2/(8\ln 2)]$, where θ_{beam} is the full-width, half maximum of the beam. The quantities ω_{T} and ω_{P} are inverse squares of the detector noise level per steradian for temperature and polarization, respectively; these can be determined by $\omega_{\mathrm{T,P}} = (\theta_{\mathrm{beam}}\sigma_{\mathrm{T,P}})^{-2}$, where σ_{T} and σ_{P} are the noise in

---

[4]In fact the BB spectrum does not add significant constraining power to either the 6-parameter ΛCDM or 7-parameter ΛCDM + T_0 models, except by noticeably improving the constraints on the dark matter density $\Omega_{\mathrm{c}}h^2$ by around a factor of 2 at $\ell_{\max} \simeq 2000$ for the 6-parameter ΛCDM model. However, the differences between the constraints for $\Omega_{\mathrm{c}}h^2$ with or without the BB spectrum become negligible by $\ell_{\max} \simeq 5000$. Most of the lensing information contained in the BB power spectrum is also contained in the EE power spectrum in the CVL case.

units of μK per full-width, half maximum beam size. For convenience, we use a single channel as a simple approximation for modeling the *Planck* results, taking values from Ref. [81], namely $\theta_{\mathrm{beam}} = 5.5$, $\sigma_{\mathrm{T}} = 11.7$ μK, and $\sigma_{\mathrm{P}} = 24.3$ μK. We have verified that this noise specification provides an excellent forecast for the current *Planck* results in [3]. We sum ℓ from 2 to 2500 with the above beam size and white noise specification, which we used to generate Fig. 1. Since the noise here is specified in μK, we use Eq. (12) to convert the dimensionless C_ℓ into μK^2 units, as described in Sec. II for CMB power spectra. Ideally, the noise should be specified as dimensionless as well and will have the same calibration as the signal; however, in practice even if the noise was calibrated differently than the signal this would make negligible difference (since changing the calibration choice will at most lead to a small difference in the noise level, and hence this is effectively a higher-order correction for parameter forecasts).

In the CVL case, we simply remove the noise term $\omega_{\mathrm{T,P}}^{-1} B_\ell^{-2}$ from the covariance matrix [Eqs. (A3)–(A8)] to obtain the correct Fisher matrix, working entirely with dimensionless C_ℓ. *Planck* has already measured most of the information from the TT power spectrum out to $\ell \simeq 2000$, and with foregrounds it seems unrealistic to push beyond $\ell \simeq 3000$ for TT [83]. However, since the foregrounds from galaxies and galaxy clusters are very weakly polarized, we should be able to measure the primary polarization anisotropies out to $\ell \simeq 5000$ and perhaps even higher [83,84]. Therefore, in our noise-free experiment, we take $\ell_{\max} = 3000$ for TT and $\ell_{\max} = 6000$ for the TE and EE power spectra in Eq. (A2). The C_ℓ power spectra become non-Gaussian at $\ell \simeq 5000$ due to the effects of lensing on small scales, so the Fisher forecast will not be exactly accurate there. However, the Fisher forecast still gives an approximate estimate of the error. Instead of providing an exact error forecast, we are mostly interested in the general effects of the FIRAS error on cosmological parameter constraints, so the use of Fisher matrix is sufficient for our purpose. Figures 2 and 5 are obtained using these CVL settings.

To combine independent likelihood functions, we can add the corresponding Fisher matrix of each likelihood function to find the total Fisher matrix, and the FIRAS prior is indeed independent of the CMB likelihood function. For a normal distribution for $T_{0,\mathrm{F}}$ with standard deviation σ_{F} that characterizes the FIRAS measurement in Eq. (1), where $\sigma_{\mathrm{F}} = 0.0006$ K is known, the T_0-T_0 term of the Fisher matrix is $1/\sigma_{\mathrm{F}}^2$; we therefore just add $1/\sigma_{\mathrm{F}}^2$ to the T_0-T_0 term in the CMB Fisher matrix calculated from Eq. (A2) to account for the FIRAS prior in the ΛCDM + T_0 model.

To study the constraining power of the lensing reconstruction spectrum $C_\ell^{\phi\phi}$ on T_0 in the CVL setting, we include $C_\ell^{\phi\phi}$ in Eq. (A2). The additional terms in the symmetric covariance matrix are given by [82]

TABLE VI. Estimated errors for BAO scale measurements in a *Euclid*-like large-scale structure survey (see Ref. [86] for further details). The first row shows the central redshift of each observational bin. The other rows give the estimated percentage error $\Delta y/y$ on the transverse and radial BAO scales, where $y^\perp(z) = D_A(z)/r_s$ and $y^\parallel(z) = H(z)r_s$, respectively.

z	0.65	0.75	0.85	0.95	1.05	1.15	1.25	1.35	1.45	1.55	1.65	1.75	1.85	1.95	2.05
$(\Delta y/y)^\perp$ [%]	1.23	0.83	0.74	0.71	0.70	0.70	0.70	0.73	0.78	0.87	1.01	1.23	1.61	2.32	5.32
$(\Delta y/y)^\parallel$ [%]	1.89	1.42	1.27	1.19	1.14	1.12	1.10	1.11	1.16	1.24	1.40	1.64	2.07	2.90	6.39

$$(\mathrm{Cov}_\ell)_{\mathrm{T}\phi} = \frac{1}{\mathcal{N}}(C_\ell^{\mathrm{T}\phi})^2, \qquad (A9)$$

$$(\mathrm{Cov}_\ell)_{\mathrm{E}\phi} = \frac{1}{\mathcal{N}}(C_\ell^{\mathrm{E}\phi})^2, \qquad (A10)$$

$$(\mathrm{Cov}_\ell)_{\mathrm{C}\phi} = \frac{1}{\mathcal{N}}C_\ell^{\mathrm{T}\phi}C_\ell^{\mathrm{E}\phi}, \qquad (A11)$$

$$(\mathrm{Cov}_\ell)_{\phi\phi} = \frac{1}{\mathcal{N}}(C_\ell^{\phi\phi})^2. \qquad (A12)$$

We take the lensing reconstruction spectrum to extend to $\ell_{\max} = 1000$ in Eq. (A2). Here the CVL condition refers to the ideal no-noise assumption for the measurement the of CMB lensing reconstruction spectrum $C_\ell^{\phi\phi}$. We exclude the actual reconstruction noise for simplicity. Figure 4 is obtained with the inclusion of $C_\ell^{\phi\phi}$ in the Fisher matrix, assuming CVL settings.

2. Fisher matrix for BAO

To break the geometric degeneracy and further constrain the late-time expansion, it is common practice to combine CMB data with BAO measurements for estimating cosmological parameters. BAO surveys generally use galaxy clustering to measure the transverse and radial scales of the sound horizon at recombination. The uncertainty in BAO experiments can be given as the errors on the transverse and radial BAO scale parameters $y^\perp(z) = D_A(z)/r_s$ and $y^\parallel(z) = H(z)r_s$, respectively. We use $\Delta y^\perp$ and $\Delta y^\parallel$ to represent the errors associated with their measurement. For simplicity, we assume that the errors in $y^\perp$ and $y^\parallel$ are uncorrelated with each other and that there are no correlations between different redshift bins. In this case, the covariance matrix is diagonal, and the full Fisher matrix for BAO simplifies to [85]

$$F_{ij}^{\mathrm{BAO}} = \sum_i \frac{1}{(\Delta y_i^\perp)^2} \frac{\partial y^\perp(z_i)}{\partial p_i} \frac{\partial y^\perp(z_i)}{\partial p_j}$$
$$+ \sum_i \frac{1}{(\Delta y_i^\parallel)^2} \frac{\partial y^\parallel(z_i)}{\partial p_i} \frac{\partial y^\parallel(z_i)}{\partial p_j}, \qquad (A13)$$

where the sums run over the observational bins at different redshifts. We take the central redshift values of each bin to calculate $y^\perp(z)$ and $y^\parallel(z)$ using CAMB. The errors forecast

for a *Euclid*-like experiment are given explicitly in Table VI, and are derived from Ref. [86], using a method based on the work of Refs. [87,88]. To combine the forecasts coming from CMB and BAO measurements, we add the Fisher matrix results from each experiment. These combined CMB and BAO forecasts are used to estimate future parameter constraints on T_0 in Sec. III C and Ω_K in Sec. IV B.

APPENDIX B: TEMPERATURE DEFINITIONS

There are several temperature-related quantities referred to in this paper. In order to distinguish between them, Table VII provides definitions and values (where appropriate) for various temperatures.

APPENDIX C: INHOMOGENEITY AND T_0

Throughout this paper we have implicitly treated T_0 as a background cosmological parameter, i.e., as spatially constant. In reality the gravitational redshifts and blueshifts due to structure change this picture, resulting in spatial as well as time dependence for the CMB temperature. A straightforward example of this is that the gravitational potential at the surface of the Earth, compared to the potential at a great distance, increases the CMB temperature on the ground by a factor $1 + GM_\oplus/R_\oplus c^2 \simeq 1 + 7 \times 10^{-10}$ over the distant value. While this is a negligible amount, structure on large scales is expected to perturb T_0 at the 10^{-5} level[5] [68], which is only of order a tenth the FIRAS uncertainty. Therefore, when we consider the ultimate effect of the T_0 uncertainty with experiments that supersede FIRAS, it will be important to take into account the inhomogeneity of the Universe.

The perturbations of the CMB temperature over constant-time slices of the spacetime result in a cosmic variance, C_0, in T_0 that was first studied for particular slices (i.e., in a particular gauge) in Ref. [90]. In Ref. [68] the result of a calculation of C_0 in comoving gauge [91] was reported and found to have a negligible effect on the uncertainties of the other cosmological parameters relative to that of the FIRAS uncertainty. Note, however, that the

---

[5]Metric perturbations caused by clusters and superclusters of galaxies are at the 10^{-5} level, this being one of the "six numbers" described by Martin Rees [89], which makes peculiar motions with kinetic energies that have v^2/c^2 of order 10^{-5}.

TABLE VII. Different temperatures and definitions used throughout this paper. T_* and T_{drag} values are taken from Table II.

Parameter	Definition	Value
$\Delta T/T$	Dimensionless CMB anisotropy. We use this schematically, with no precise meaning for the denominator.	$\cdots$
ΔT_{RJ}	Rayleigh-Jeans temperature fluctuation, $\Delta I_\nu c^2/2k\nu^2$.	$\cdots$
T_0	Present-day temperature of the photon background, or the monopole term in the spherical-harmonic expansion of the CMB sky.	$\cdots$
$T_{0,F}$	Current CMB monopole temperature measurement, derived by *COBE*-FIRAS combined with other experiments.	(2.7255 ± 0.0006) K
$\bar{T}_{0,F}$	Central value for current monopole temperature measurement (i.e., the FIRAS measurement), often used as the calibration temperature.	2.7255K
T_c	Arbitrary fixed (errorless) calibration temperature, used to convert dimensionless power spectra to temperature units. Often set to $\bar{T}_{0,F}$.	$\cdots$
T_γ, $T_\gamma(z)$	Photon temperature at redshift z. $T_0 = T_\gamma(z=0)$.	$\cdots$
T_*	Temperature at the epoch of last scattering, fixed by the physics of recombination. $T_* = T_\gamma(z_*)$. Value from this work and Ref. [3].	(2973.27 ± 0.67) K
T_e	Kinetic temperature of the electrons.	$\cdots$
T_{drag}	Temperature at the Compton drag epoch. $T_{drag} = T_\gamma(z_{drag})$. Value from this work and Ref. [3].	(2891.60 ± 0.78) K

choice of gauge in these studies was arbitrary, and can lead to a zero, order 10^{-5}, or divergent result for C_0 [90]. For an eventual successor to FIRAS, we note that the effect of super-Hubble fluctuations in T_0 should be irrelevant insofar as the effect on the cosmological parameters within our Hubble volume is concerned. We also point out that the perturbations due to sub-Hubble structure could, in principle, be taken into account and corrected for by mapping that structure. So ultimately we do not expect the cosmic variance of T_0 to have an important effect on the determinations of the other parameters.

In further work related to the effect of inhomogeneity on the CMB temperature, Ref. [41] notes that by varying the spatial curvature parameter Ω_K as well as T_0, tensions with the Hubble and other parameters can be reduced even when including BAO data, due to the extra freedom in the background evolution that curvature allows. At roughly 10% the required shift in T_0 is still much larger than the FIRAS uncertainty, although the authors of Ref. [41] claim this can be explained by our presence in a large underdensity, which would render the locally measured T_0 colder than outside the void. However, as mentioned above the gravitational redshift or blueshift due to realistic structure is of order 10^{-5} over a large range of scales. Thus the proposal of [41] would require a potential well that is four orders of magnitude deeper than expected, likely conflicting with a range of observations [45].

[1] Planck Collaboration XVI, Astron. Astrophys. **571**, A16 (2014).

[2] Planck Collaboration XIII, Astron. Astrophys. **594**, A13 (2016).

[3] Planck Collaboration VI, Astron. Astrophys. **641**, A6 (2020).

[4] G. Hinshaw, D. Larson, E. Komatsu, D. N. Spergel, C. L. Bennett *et al.*, Astrophys. J. Suppl. Ser. **208**, 19 (2013).

[5] S. Aiola, E. Calabrese, L. Maurin *et al.*, J. Cosmol. Astropart. Phys. 12 (2020) 047.

[6] D. J. Fixsen, E. S. Cheng, J. M. Gales, J. C. Mather, R. A. Shafer, and E. L. Wright, Astrophys. J. **473**, 576 (1996).

[7] D. J. Fixsen, Astrophys. J. **707**, 916 (2009).

[8] B. A. Benson, P. A. R. Ade, Z. Ahmed, S. W. Allen, K. Arnold *et al.*, in *Millimeter, Submillimeter, and Far-Infrared Detectors and Instrumentation for Astronomy VII*, Society of Photo-Optical Instrumentation Engineers (SPIE) Conference Series, Vol. 9153 (2014), p. 91531P [arXiv:1407.2973].

[9] S. Naess, M. Hasselfield, J. McMahon, M. D. Niemack, G. E. Addison *et al.*, J. Cosmol. Astropart. Phys. 10 (2014) 007.

[10] K. N. Abazajian, P. Adshead, Z. Ahmed, S. W. Allen, D. Alonso *et al.*, arXiv:1610.02743.

[11] E. Di Valentino *et al.*, J. Cosmol. Astropart. Phys. 04 (2018) 017.

[12] A. Lewis, A. Challinor, and A. Lasenby, Astrophys. J. **538**, 473 (2000).

[13] D. Blas, J. Lesgourgues, and T. Tram, J. Cosmol. Astropart. Phys. 07 (2011) 034.

[14] P. J. E. Peebles, Astrophys. J. **142,** 1317 (1965).
[15] R. K. Sachs and A. M. Wolfe, Astrophys. J. **147,** 73 (1967).
[16] J. Silk, Nature (London) **218,** 453 (1968).
[17] R. A. Sunyaev and Y. B. Zeldovich, Astrophys. Space Sci. **7,** 3 (1970).
[18] M. M. Ivanov, Y. Ali-Haïmoud, and J. Lesgourgues, Phys. Rev. D **102,** 063515 (2020).
[19] Planck Collaboration V, Astron. Astrophys. **641,** A5 (2020).
[20] J. P. Zibin, A. Moss, and D. Scott, Phys. Rev. D **76,** 123010 (2007).
[21] Planck Collaboration VIII, Astron. Astrophys. **594,** A8 (2016).
[22] F. Pajot, P. A. R. Ade, J. L. Beney, E. Bréelle, D. Broszkiewicz *et al.,* Astron. Astrophys. **520,** A10 (2010).
[23] Planck Collaboration V, Astron. Astrophys. **571,** A5 (2014).
[24] Planck Collaboration VIII, Astron. Astrophys. **571,** A8 (2014).
[25] Planck Collaboration V, Astron. Astrophys. **594,** A5 (2016).
[26] Planck Collaboration II, Astron. Astrophys. **641,** A2 (2020).
[27] Planck Collaboration III, Astron. Astrophys. **641,** A3 (2020).
[28] B. Bertincourt, G. Lagache, P. G. Martin, B. Schulz, L. Conversi *et al.,* Astron. Astrophys. **588,** A107 (2016).
[29] H. K. Eriksen *et al.,* Astrophys. J. **641,** 665 (2006).
[30] A. Kogut and D. J. Fixsen, J. Cosmol. Astropart. Phys. 05 (2020) 041.
[31] P. André, C. Baccigalupi, A. Banday, D. Barbosa, B. Barreiro *et al.,* J. Cosmol. Astropart. Phys. 02 (2014) 006.
[32] Planck Collaboration I, Astron. Astrophys. **641,** A1 (2020).
[33] Planck Collaboration Int. LVII, Astron. Astrophys. **643,** A42 (2020).
[34] Beyond Planck Collaboration I, arXiv:2011.05609.
[35] G. Ye (private communication).
[36] J. Lesgourgues (private communication).
[37] G. Ye and Y.-S. Piao, Phys. Rev. D **102,** 083523 (2020).
[38] W. Hu, D. Scott, N. Sugiyama, and M. White, Phys. Rev. D **52,** 5498 (1995).
[39] J. Chluba and R. A. Sunyaev, Astron. Astrophys. **478,** L27 (2008).
[40] J. Hamann and Y. Y. Y. Wong, J. Cosmol. Astropart. Phys. 03 (2008) 025.
[41] B. Bose and L. Lombriser, Phys. Rev. D **103,** L081304 (2021).
[42] A. Moss, J. P. Zibin, and D. Scott, Phys. Rev. D **77,** 043505 (2008).
[43] A. Narimani, A. Moss, and D. Scott, Astrophys. Space Sci. **341,** 617 (2012).
[44] A. Lewis and A. Challinor, Phys. Rep. **429,** 1 (2006).
[45] A. Moss, J. P. Zibin, and D. Scott, Phys. Rev. D **83,** 103515 (2011).
[46] D. Scott and A. Moss, Mon. Not. R. Astron. Soc. **397,** 445 (2009).
[47] P. J. E. Peebles, Astrophys. J. **153,** 1 (1968).
[48] Y. B. Zeldovich, V. G. Kurt, and R. A. Syunyaev, Zh. Eksp. Teor. Fiz. **55,** 278 (1968).
[49] J. Chluba and R. M. Thomas, Mon. Not. R. Astron. Soc. **412,** 748 (2011).
[50] Y. Ali-Haïmoud and C. M. Hirata, Phys. Rev. D **83,** 043513 (2011).

[51] D. N. Spergel, L. Verde, H. V. Peiris, E. Komatsu, M. R. Nolta *et al.,* Astrophys. J. Suppl. Ser. **148,** 175 (2003).
[52] W. Hu, ASP Conf. Ser. **339,** 215 (2005).
[53] M. Shimon and Y. Rephaeli, Phys. Rev. D **102,** 083532 (2020).
[54] W. Hu and N. Sugiyama, Astrophys. J. **471,** 542 (1996).
[55] J. Torrado and A. Lewis, J. Cosmol. Astropart. Phys. 05 (2021) 057.
[56] S. Seager, D. D. Sasselov, and D. Scott, Astrophys. J. **523,** L1 (1999).
[57] S. Seager, D. D. Sasselov, and D. Scott, Astrophys. J. Suppl. Ser. **128,** 407 (2000).
[58] Planck Collaboration, Int. LI, Astron. Astrophys. **607,** A95 (2017).
[59] K. M. Smith, W. Hu, and M. Kaplinghat, Phys. Rev. D **74,** 123002 (2006).
[60] S. Alam, M. Ata, S. Bailey, F. Beutler, D. Bizyaev *et al.,* Mon. Not. R. Astron. Soc. **470,** 2617 (2017).
[61] DESI Collaboration, arXiv:1611.00036.
[62] Euclid Collaboration, Astron. Astrophys. **642,** A191 (2020).
[63] R. Laureijs, J. Amiaux, S. Arduini, J. L. Auguères, J. Brinchmann *et al.,* arXiv:1110.3193.
[64] A. G. Riess, S. Casertano, W. Yuan, L. M. Macri, and D. Scolnic, Astrophys. J. **876,** 85 (2019).
[65] H. P. Gush, M. Halpern, and E. H. Wishnow, Phys. Rev. Lett. **65,** 537 (1990).
[66] R. Salvaterra and C. Burigana, Construction of a database of CMB spectrum observations, Technical Report No. ITeSRE/CNR/270/2000, Istituto Tecnologie e Studio Radiazioni Extraterrestri, Bologna, Italy, 2002, arXiv:astro-ph/0206350].
[67] A. C. Hall and A. Challinor, Mon. Not. R. Astron. Soc. **425,** 1170 (2012).
[68] J. Yoo, E. Mitsou, Y. Dirian, and R. Durrer, Phys. Rev. D **100,** 063510 (2019).
[69] M. H. Abitbol, J. Chluba, J. C. Hill, and B. R. Johnson, Mon. Not. R. Astron. Soc. **471,** 1126 (2017).
[70] A. Kogut, M. H. Abitbol, J. Chluba, J. Delabrouille, D. Fixsen, J. C. Hill, S. P. Patil, and A. Rotti, in Bulletin of the American Astronomical Society, Vol. **51** (2019), p. 113 [arXiv:1907.13195].
[71] J. Chluba, M. H. Abitbol, N. Aghanim, Y. Ali-Haimoud, M. Alvarez, K. Basu *et al.,* arXiv:1909.01593.
[72] www.computecanada.ca.
[73] www.esa.int/Planck.
[74] camb.readthedocs.io/en/latest/.
[75] cobaya.readthedocs.io/en/latest/.
[76] www.astro.ubc.ca/people/scott/recfast.html.
[77] R. A. Fisher, Phil. Trans. R. Soc. A **222,** 309 (1922).
[78] M. Tegmark, A. N. Taylor, and A. F. Heavens, Astrophys. J. **480,** 22 (1997).
[79] A. Heavens, arXiv:0906.0664.
[80] D. Coe, arXiv:0906.4123.
[81] D. J. Eisenstein, W. Hu, and M. Tegmark, Astrophys. J. **518,** 2 (1999).
[82] L. Santos, P. Cabella, A. Balbi, and N. Vittorio, Phys. Rev. D **88,** 043505 (2013).
[83] D. Scott, D. Contreras, A. Narimani, and Y.-Z. Ma, J. Cosmol. Astropart. Phys. 06 (2016) 046.

[84] G. Simard, D. Hanson, and G. Holder, Astrophys. J. **807,** 166 (2015).

[85] N. A. Lima, P. T. P. Viana, and I. Tereno, Mon. Not. R. Astron. Soc. **441,** 3231 (2014).

[86] A. Font-Ribera, P. McDonald, N. Mostek, B. A. Reid, H.-J. Seo, and A. Slosar, J. Cosmol. Astropart. Phys. 05 (2014) 023.

[87] H.-J. Seo and D. J. Eisenstein, Astrophys. J. **598,** 720 (2003).

[88] H.-J. Seo and D. J. Eisenstein, Astrophys. J. **665,** 14 (2007).

[89] M. J. Rees, *Just Six Numbers: The Deep Forces that Shape The Universe* (Weidenfeld & Nicolson, London, 1999).

[90] J. P. Zibin and D. Scott, Phys. Rev. D **78,** 123529 (2008).

[91] S. Baumgartner and J. Yoo, Phys. Rev. D **103,** 063516 (2021).